AIMS Mathematics, 11(3): 6106–6140.
DOI: 10.3934/math.2026253
Received: 30 January 2026
Revised: 03 March 2026
Accepted: 4 March 2026
Published: 11 March 2026

http://www.aimspress.com/journal/Math

Research article

Reliability inference of the quadratic hazard rate model under step-stress partially accelerated life testing with progressive Type-II censoring

Hanan Haj Ahmad[1,*], Moustafa N. Mousa[2], M. E. Moshref[3], N. Youns[2] and Mahmoud M. M. Mansour[4]

[1] Department of Mathematics and Statistics, College of Science, King Faisal University, Hofuf 31982, Al-Ahsa, Saudi Arabia
[2] Department of Mathematics, Faculty of Science, Kafrelsheikh University, Kafrelsheikh 33516, Egypt
[3] Department of Mathematics, Faculty of Science, Al-Azhar University, Nasr City 11884, Cairo, Egypt
[4] Department of Basic Science, Faculty of Engineering, The British University in Egypt, El Sherouk City, Cairo, Egypt

* **Correspondence:** Email: hhajahmed@kfu.edu.sa.

Abstract: Step-stress partially accelerated life testing (SSPALT) provides an effective framework for obtaining timely reliability information when products operate under varying stress levels. In this paper, statistical inference and applications of the quadratic hazard rate distribution are developed under SSPALT with progressive Type-II censoring and binomial removals. This censoring scheme offers flexibility in balancing the experimental cost and statistical efficiency while accommodating practical testing constraints. Maximum likelihood and Bayesian estimation are derived for the model parameters and the acceleration factor. Computational implementations are carried out using the Markov chain Monte Carlo method. Reliability analyses, including survival and hazard rate functions, are carried out to support practical reliability assessment and decision-making. Asymptotic confidence intervals and credible intervals are constructed to quantify the estimation uncertainty. The performance of the proposed estimators is evaluated through Monte Carlo simulations under different experimental settings. The methodology is illustrated using three real data sets from solar lighting equipment, nanocrystalline devices, and micro-unmanned aerial vehicles. The results emphasize the flexibility and accurate inference for accelerated reliability testing, making it suitable for a wide range of applications.

Keywords: accelerated life testing; quadratic hazard rate; progressive censoring; maximum likelihood; Bayesian inference; reliability analysis

Mathematics Subject Classification: 60G35, 62F10, 62F15, 62N01, 62N02, 62N05

1. Introduction

Driven by ever-increasing market expectations and rapid technological progress, manufacturers require methods that are capable of providing reliable lifetime estimates within a reduced time frame compared with conventional life testing (CLT). Despite the critical role CLT techniques play in evaluations of reliability, they are time-consuming and expensive, especially in products that have high reliability. To overcome these limitations, accelerated life testing (ALT) has been created as an efficient method of statistically based reliability testing (SRT). In ALT, test units are exposed to a high level of stress, which can be temperature, voltage, humidity, vibration, or pressure, to cause failures faster. The observed data are then extrapolated to normal operating conditions through an assumed life-stress relationship. The foundations of ALT have been established by Bessler et al. [1], Chernoff [2], and developed further by Nelson [3], Meeker et al. [4], Han and Bai [5], and Rahman et al. [6]. Several types of stress-loading patterns have been commonly used in ALT experiments, as illustrated in Figure 1.

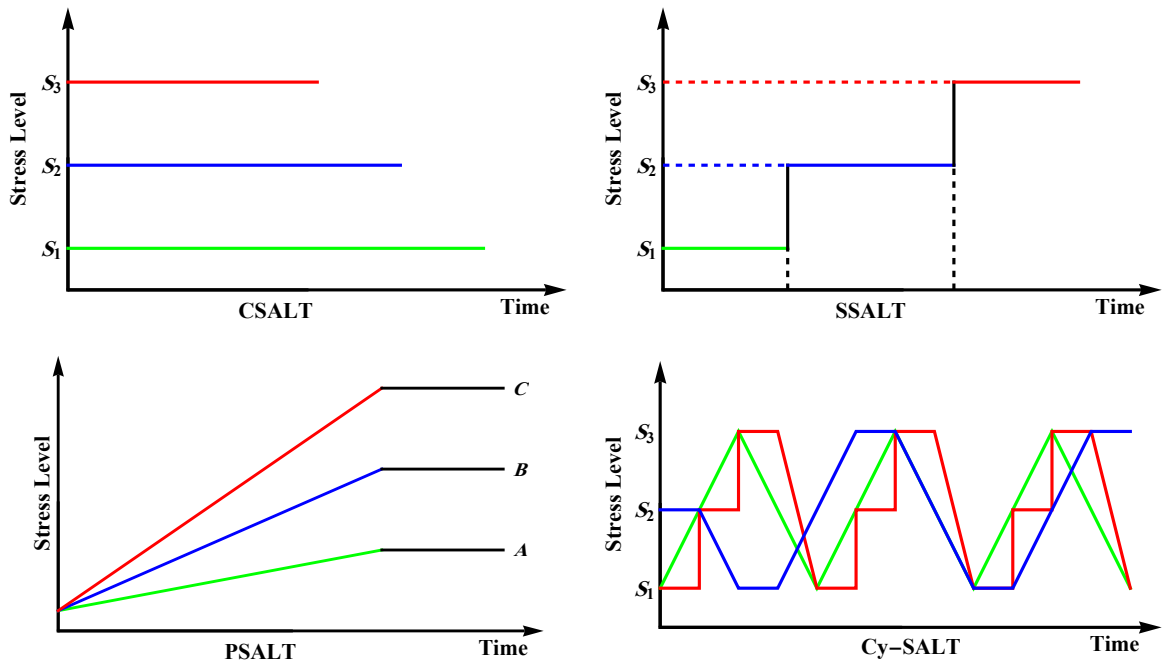

Figure 1. Various patterns of accelerated stress loadings in ALT.

These types include:

- Constant-stress ALT (CSALT): A fixed stress level is maintained throughout the experiment, providing a simple design and analysis framework.
- Step-stress ALT (SSALT): The stress level changes at predetermined times or failure instances, allowing a more informative estimation of the life-stress relationship.

- Progressive stress ALT (PSALT): Stress is continuously increased over time, offering a realistic representation of gradual degradation.
- Cyclic-stress ALT (Cy-SALT): The stress varies periodically to mimic real-life operational environments, such as thermal or mechanical cycling.

A complete ALT design requires the specification of (i) the stress profile and timing, (ii) the allocation of test units across stress levels, and (iii) the life-stress relationship used for extrapolation. In situations where a valid life-stress model is not available, partially accelerated life testing (PALT) is used. In PALT, units are tested under both normal and elevated stress levels to estimate the acceleration factor (AF) empirically. The two main variants of PALT are:

- Constant stress PALT (CSPALT): Each unit is tested at a fixed stress level until failure or censoring.
- Step-stress PALT (SSPALT): Units are initially operated under normal conditions for a specified period, after which the stress level is increased stepwise, and the test continues until failure or censoring.

Along with the design of the stress-loading schemes, the treatment of incomplete observations through censoring plays a fundamental role in reliability experiments. In a wide variety of applications, lifetime data are not observable over an item's entire life because of time, cost, or experimental limitations. In this case, censoring schemes are used to effectively utilize the available information. A lifetime observation is considered to be censored when the actual time of failure is unknown, although partial information about its occurrence is available. ALT and PALT experiments frequently incorporate censoring methods to minimize the duration of testing while maintaining statistical efficiency.

Among the classical censoring schemes, Type I censoring (time censoring) has been defined by terminating the experiment at a prespecified time, with all surviving units treated as censored observations. Although this scheme is simple to implement, it may yield insufficient failure information if the test duration is not properly chosen. Alternatively, Type II censoring (failure censoring) has been defined by continuing the experiment until a prefixed number of failures is observed, ensuring an adequate amount of failure data. Nevertheless, it can result in too-long experiments in situations where there are few instances of failure. To overcome these limitations, the progressive Type II censoring scheme (P-T-II CS) has been proposed as a flexible extension of classical censoring designs. Under this scheme, units are progressively removed from the experiment at each observed failure time.

Specifically, after the occurrence of the ith failure, a predetermined or random number of surviving units are withdrawn from the test. This mechanism allows the experimenter to control the number of units under observation, thereby balancing statistical precision and experimental cost. To facilitate an understanding of this mechanism, a schematic illustration of the P-T-II CS is presented in Figure 2.

As illustrated in Figure 2, the experiment begins with n units placed in the test. When the first failure occurs at time $y_{1:m:n}$, r_1 surviving units are removed from the remaining units. This process continues sequentially such that, at each failure time $y_{i:m:n}$, r_i units are withdrawn. The experiment continues until the mth failure is observed, at which point the test is terminated.

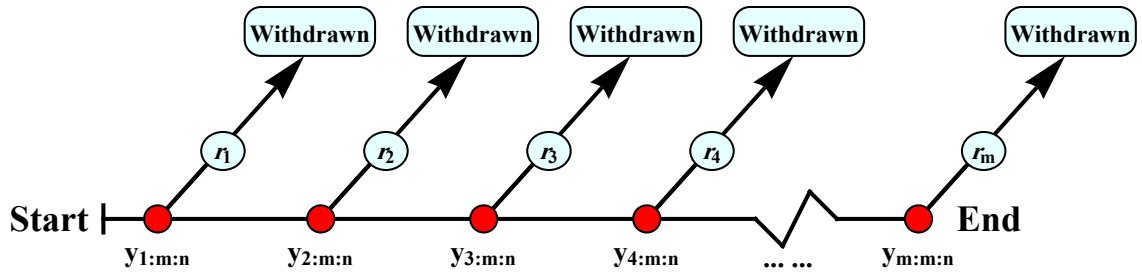

Figure 2. Illustration of the P-T-II CS.

A further extension of the progressive censoring framework has been achieved through the incorporation of binomial removals. In this approach, the number of units removed at each failure time is treated as a random variable. In particular, if n units are initially placed on a test and m failures are observed, then after the ith failure at time $y_{i:m:n}$, the number of withdrawn units r_i is assumed to follow a binomial distribution given by $r_i \sim \text{binomial}\left(n - m - \sum_{j=1}^{i-1} r_j,\ p\right)$, subject to the constraint $\sum_{i=1}^{m} r_i = n - m$, where p denotes the removal probability. This stochastic removal mechanism enhances the flexibility of the censoring scheme and allows for more realistic modeling of experimental conditions.

It is worth noting that several classical censoring schemes arise as special cases of the progressive censoring framework. For example, the complete sample case is obtained when no units are removed during the experiment (i.e., $r_i = 0$ for all i and $m = n$), while the traditional Type II censoring scheme is recovered when removals occur only at the final failure (i.e., $r_i = 0$ for $i < m$ and $r_m = n - m$), as discussed by Wu [7].

The literature indicates that a considerable number of studies have addressed parameter estimation under the P-T-II CSs. Notable contributions include Ahmed [8], Mahmoud et al. [9], Wang et al. [10], Ramadan et al. [11], Tashkandy et al. [12], Haj Ahmad [13], and Abo-Kasem et al. [14]. In parallel, the SSPALT framework has been investigated under various censoring mechanisms by Bai et al. [15], Rahman et al. [16], El-Sagheer et al. [17], Alam et al. [18], Al-Essa et al. [19], Manal et al. [20], Alam and Ahmed [21], Yousef et al. [22], Tian and Gui [23], and Ahmad et al. [24].

The selection of an appropriate lifetime distribution is crucial in reliability modeling. In this study, the three-parameter quadratic hazard rate distribution (QHRD), introduced by Bain [25], is considered due to its flexibility in modeling increasing, decreasing, and non-monotonic hazard rate shapes. The QHRD has been studied further by Elbatal and Butt [26], Mustafa [27], Bhatti et al. [28], Merovci and Elbatal [29], Okasha et al. [30], and Al-Hossain and Dar [31].

Although several studies have investigated ALT models and progressive censoring schemes, most have focused on classical lifetime distributions such as the exponential, Weibull, Lomax, or Marshall-Olkin families under SSPALT settings. In contrast, existing works on the QHRD have primarily assumed complete or simply censored samples, without considering accelerated testing conditions or complex censoring mechanisms.

The current research seeks to overcome such shortcomings by introducing a single model that combines the QHRD, SSPALT, P-T-II CS, and binomial removals, as well as the tampered random

variable (TRV) model. The QHRD is considered due to its adaptability in the effort to incorporate various behaviors of hazard rates, whereas the SSPALT design offers a real-life model of different stress situations. The P-T-II CS is efficient in terms of the experiment, and the TRV model is effective in explaining changes in lifetime distributions and stress levels. This framework has been developed via both classical maximum likelihood (ML) and Bayesian inferential procedures, including asymptotic confidence intervals (ACIs) and highest posterior density (HPD) for credible intervals (CRIs), and this was obtained through Markov chain Monte Carlo (MCMC) methods. To the best of our knowledge, no previous study has simultaneously combined the QHRD, SSPALT, the P-T-II CS with binomial removals, and the TRV modeling framework under both classical and Bayesian paradigms. Therefore, the present work provides a comprehensive extension of the existing literature, both methodologically and computationally.

The main objectives of this study are as follows.

(1) Estimate the parameters of the QHRD and the acceleration factor under SSPALT with the P-T-II CS and binomial removals.
(2) Derive and analyze the associated reliability and hazard rate functions to evaluate:
   (a) The probability that a unit surviving up to time t continues to survive for an additional time interval;
   (b) The instantaneous failure risk given that survival occurs up to time t.

The remainder of this paper is organized as follows. Section 2 presents the QHRD and describes the SSPALT procedure under the P-T-II CS. Section 3 develops the ML and Bayesian estimation methods, including MCMC implementations. Section 4 constructs ACIs and CRIs. Section 5 provides applications to real datasets. Section 6 presents the results of the Monte Carlo simulation, and Section 7 concludes the paper.

2. Model description under SSPALT with the P-T-II CS

Let Y be a non-negative continuous lifetime variable following the QHRD. Its probability density function (PDF) and cumulative distribution function (CDF) can be written as

$$f(y;\alpha,\beta,\lambda) = (\alpha+\beta y+\lambda y^2)\, e^{-\left(\alpha y+\frac{\beta}{2}y^2+\frac{\lambda}{3}y^3\right)} \quad \text{and} \quad F(y;\alpha,\beta,\lambda) = 1-e^{-\left(\alpha y+\frac{\beta}{2}y^2+\frac{\lambda}{3}y^3\right)}. \tag{2.1}$$

Accordingly, the reliability function (RF) and hazard function (HF) are written as

$$R(y;\alpha,\beta,\lambda) = e^{-\left(\alpha y+\frac{\beta}{2}y^2+\frac{\lambda}{3}y^3\right)} \quad \text{and} \quad h(y;\alpha,\beta,\lambda) = \left(\alpha+\beta y+\lambda y^2\right). \tag{2.2}$$

To ensure the non-negativity of the HF, we assume $\alpha \geq 0$, $\lambda \geq 0$, and $\beta \geq -2\sqrt{\alpha\,\lambda}$. Under these constraints, the QHRD provides considerable flexibility in modeling lifetime data, admitting various shapes as detailed in Nagy et al. [32] and Mousa et al. [33].

Figure 3 illustrates the flexibility of the QHRD model. Since the HF is quadratic, its shape is governed directly by the parameters. When $\beta \geq 0$ and $\lambda \geq 0$, the hazard is monotone increasing, representing aging behavior. When $\beta < 0$ and $\lambda = 0$, the hazard decreases linearly while remaining positive under the admissibility conditions. For $\beta < 0$ and $\lambda > 0$, the quadratic structure produces a bathtub-shaped hazard with a turning point at $y^* = -\frac{\beta}{2\lambda}$. The corresponding density functions reflect

these behaviors, confirming that the QHRD accommodates increasing, decreasing, and non-monotonic hazard patterns within a unified three-parameter framework. In addition, the QHRD includes a number of well-known lifetime distributions as special cases, which further underlines its generality. Specifically, it reduces to the linear hazard rate distribution (LHRD) when $\lambda = 0$. When the two parameters are $\beta = 0$ and $\lambda = 0$, it ultimately leads to the exponential distribution (ED), with a fixed hazard rate. Moreover, at the point of $\alpha = 0$ and $\lambda = 0$, the model is equal to the Rayleigh distribution (RD). These special cases demonstrate that the QHRD provides a comprehensive extension of classical models, offering enhanced flexibility for modeling diverse reliability behaviors while retaining important standard distributions as particular instances.

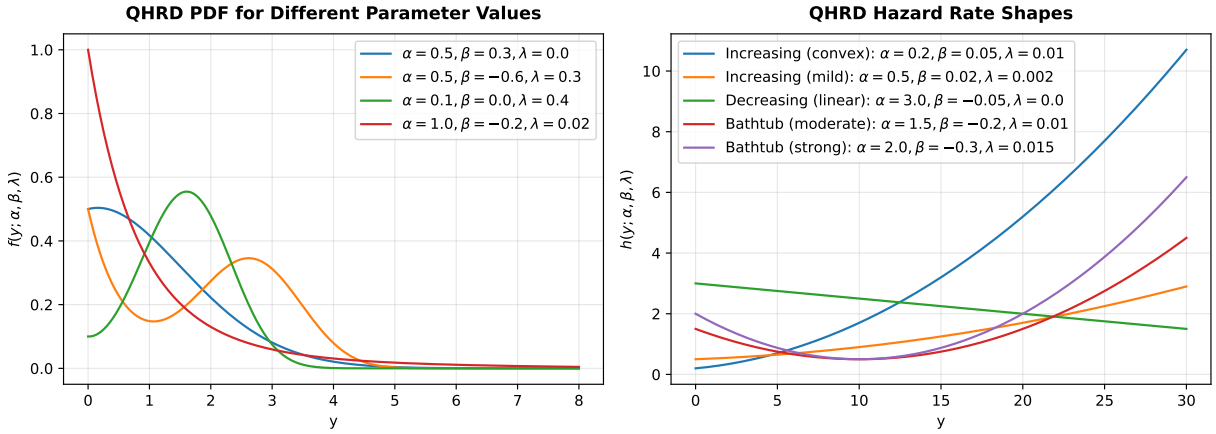

Figure 3. PDF (left) and HF (right) of the QHRD.

The life test under the SSPALT with the P-T-II CS proceeds as follows.

(1) Test initialization: At time zero, place n units each with lifetime $T \sim \text{QHRD}(\alpha, \beta, \lambda)$ and assumed to be identically and independently distributed (*i.i.d.*) into the test. Only the first m failures ($m \leq n$) are to be observed; denote their ordered lifetimes as $y_{1:m:n} \leq y_{2:m:n} \leq \cdots \leq y_{m:m:n}$.

(2) Stress application: All units begin under normal stress. At a predetermined time τ, elevate the stress to the accelerated level.

(3) Failure recordings and withdrawals.

- Whenever the ith failure occurs ($i = 1, \ldots, m$), record $y_{i:m:n}$.
- Immediately after each recorded failure (for $i < m$), withdraw r_i survivors at random.
- Once there are m failures, discard the other $r_m = n - m - \sum_{i=1}^{m-1} r_i$ units, and the test is over.

(4) Random censoring mechanism. Each withdrawal count r_i follows a binomial model reflecting the independent removal probability p. In particular,

$$r_1 \sim \text{binomial}\,(n - m,\ p)\,, \quad r_i \sim \text{binomial}\left(n - m - \sum_{j=1}^{i-1} r_j,\ p\right), \quad i = 2, \ldots, m.$$

(5) TRV-based lifetime transformation. In order to model the stress change at τ, we adopt the TRV model of Goel [34]. If T is the original lifetime under normal stress and $\xi > 1$ is the AF, then the

observed lifetime Y is

$$Y = \begin{cases} T, & T \leq \tau, \\ \tau + \dfrac{T-\tau}{\xi}, & T > \tau. \end{cases} \tag{2.3}$$

The resulting PDF, CDF, RFs, and HFs based on the TRV model are specified in Eq (2.3) are

$$f(y;\alpha,\beta,\lambda,\xi) = \begin{cases} f_1(y;\alpha,\beta,\lambda) = (\alpha+\beta y+\lambda y^2)e^{-\left(\alpha y+\frac{\beta}{2}y^2+\frac{\lambda}{3}y^3\right)}, & 0 < y \leq \tau, \\ f_2(y;\alpha,\beta,\lambda,\xi) = \xi(\alpha+\beta\psi(y)+\lambda\psi(y)^2)e^{-\left(\alpha\psi(y)+\frac{\beta}{2}\psi(y)^2+\frac{\lambda}{3}\psi(y)^3\right)}, & y > \tau, \end{cases} \tag{2.4}$$

$$F(y;\alpha,\beta,\lambda,\xi) = \begin{cases} F_1(y;\alpha,\beta,\lambda) = 1-e^{-\left(\alpha y+\frac{\beta}{2}y^2+\frac{\lambda}{3}y^3\right)}, & 0 < y \leq \tau, \\ F_2(y;\alpha,\beta,\lambda,\xi) = 1-e^{-\left(\alpha\psi(y)+\frac{\beta}{2}\psi(y)^2+\frac{\lambda}{3}\psi(y)^3\right)}, & y > \tau, \end{cases} \tag{2.5}$$

$$R(y;\alpha,\beta,\lambda,\xi) = \begin{cases} R_1(y;\alpha,\beta,\lambda) = e^{-\left(\alpha y+\frac{\beta}{2}y^2+\frac{\lambda}{3}y^3\right)}, & 0 < y \leq \tau, \\ R_2(y;\alpha,\beta,\lambda,\xi) = e^{-\left(\alpha\psi(y)+\frac{\beta}{2}\psi(y)^2+\frac{\lambda}{3}\psi(y)^3\right)}, & y > \tau, \end{cases} \tag{2.6}$$

$$h(y;\alpha,\beta,\lambda,\xi) = \begin{cases} h_1(y;\alpha,\beta,\lambda) = \alpha+\beta y+\lambda y^2, & 0 < y \leq \tau, \\ h_2(y;\alpha,\beta,\lambda,\xi) = \xi(\alpha+\beta\psi(y)+\lambda\psi(y)^2), & y > \tau, \end{cases} \tag{2.7}$$

respectively, where $\psi(y) = \tau + \xi(y-\tau)$.

Let the ordered failure times of P-T-II be denoted as $y_{1:m:n} < y_{2:m:n} < \cdots < y_{m:m:n}$, and suppose that a stress-change occurs at time τ, splitting the sample into two phases: Failures up to τ (normal stress) correspond to indices $i = 1,\ldots,n_1$, and failures after τ (accelerated stress) correspond to $i = n_1+1,\ldots,m$. The two indicator variables are described as follows:

$$\delta_{i,1} = \begin{cases} 1, & i \leq n_1, \\ 0, & i > n_1, \end{cases} \quad \text{(normal)} \quad \text{and} \quad \delta_{i,2} = \begin{cases} 1, & i > n_1, \\ 0, & i \leq n_1, \end{cases} \quad \text{(accelerated)}$$

so that $n_1 = \sum_{i=1}^{m} \delta_{i,1}$, $n_2 = m - n_1 = \sum_{i=1}^{m} \delta_{i,2}$. The likelihood of the parameters $\Theta = (\alpha,\beta,\lambda,\xi)$ under P-T-II CS can be expressed as explained by Balakrishnan and Aggarwala [35], Balakrishnan and Cramer [36], and Balakrishnan [37] as follows:

$$\mathcal{L}(\Theta) = c_{m-1}\prod_{i=1}^{m}\left\{f_1(y_{i:m:n};\alpha,\beta,\lambda)R_1(y_{i:m:n};\alpha,\beta,\lambda)^{r_i}\right\}^{\delta_{i,1}}\left\{f_2(y_{i:m:n};\alpha,\beta,\lambda,\xi)R_2(y_{i:m:n};\alpha,\beta,\lambda,\xi)^{r_i}\right\}^{\delta_{i,2}}, \tag{2.8}$$

where $c_{m-1} = n\,(n-r_1-1)\left(n-\sum_{i=1}^{2}(r_i+1)\right)\cdots\left(n-\sum_{i=1}^{m-1}(r_i+1)\right)$ captures the combinatorial aspect of the censoring mechanism. If we also use $P(R=r)$ to denote the joint probability of the removal counts $\{r_i\}$ illustrated by Tse et al. [38], then the joint likelihood becomes $\mathcal{L}_1(\Theta,p) = \mathcal{L}(\Theta)\times P(R=r)$, with

$$P(R=r) = \frac{(n-m)!}{\prod_{i=1}^{m-1} r_i!\,(n-m-\sum_{i=1}^{m-1} r_i)!}\; p^{\sum_{i=1}^{m-1} r_i}(1-p)^{(m-1)(n-m)-\sum_{i=1}^{m-1}(m-i)r_i}.$$

Since $\mathcal{L}(\Theta)$ does not involve p, the ML estimator of p follows by maximization of $P(R=r)$, yielding

$$\hat{p} = \frac{\sum_{i=1}^{m-1} r_i}{(m-1)(n-m) \;-\; \sum_{i=1}^{m-1}(m-i-1)\,r_i}.$$

Simply, the maximum likelihood estimates (MLEs) involving $\Theta = (\alpha,\beta,\lambda,\xi)$ are obtained by maximizing $\mathcal{L}(\Theta)$.

3. Point estimation under SSPALT with the P-T-II CS

In this section, we obtain point estimates for the QHRD parameters and the associated AF, RF, and HF via ML and Bayesian frameworks. The efficiency and the accuracy of these estimators are examined through simulation, as illustrated in Section 6.

3.1. Maximum likelihood estimation

Let $y_{i:m:n}$ (abbreviated $y_{i:m}$) denote the ordered failure times with n units under a P-T-II CS with the predetermined removals r_i, $i=1,\ldots,m$. Through the combination of Eqs (2.4)–(2.8), the likelihood can be presented as

$$\begin{aligned}\mathcal{L} = c_{m-1}\prod_{i=1}^{m}&\left\{\left(\alpha+\beta y_{i:m}+\lambda y_{i:m}^2\right)^{\delta_{i,1}} e^{-\delta_{i,1}(r_i+1)\left(\alpha y_{i:m}+\frac{\beta}{2}y_{i:m}^2+\frac{\lambda}{3}y_{i:m}^3\right)}\right\}\\ &\times\left\{\xi^{\delta_{i,2}}\left[\alpha+\beta\,\psi(y_{i:m})+\lambda\,(\psi(y_{i:m}))^2\right]^{\delta_{i,2}} e^{-\delta_{i,2}(r_i+1)\left[\alpha\,\psi(y_{i:m})+\frac{\beta}{2}(\psi(y_{i:m}))^2+\frac{\lambda}{3}(\psi(y_{i:m}))^3\right]}\right\},\end{aligned} \tag{3.1}$$

where $\psi(y_{i:m}) = \tau+\xi\,(y_{i:m}-\tau)$. Taking the natural logarithm on both sides, we have

$$\begin{aligned}\ell = \ln(c_{m-1}) + n_2\ln(\xi) &+ \sum_{i=1}^{m}\delta_{i,1}\ln\left(\alpha+\beta y_{i:m}+\lambda y_{i:m}^2\right) - \sum_{i=1}^{m}\delta_{i,1}(r_i+1)(\alpha y_{i:m}+\frac{\beta}{2}y_{i:m}^2+\frac{\lambda}{3}y_{i:m}^3)\\ &+\sum_{i=1}^{m}\delta_{i,2}\ln\left[\alpha+\beta\,\psi(y_{i:m})+\lambda\,(\psi(y_{i:m}))^2\right] - \sum_{i=1}^{m}\delta_{i,2}(r_i+1)\left[\alpha\,\psi(y_{i:m})+\frac{\beta}{2}\,(\psi(y_{i:m}))^2+\frac{\lambda}{3}\,(\psi(y_{i:m}))^3\right].\end{aligned}$$

Setting $\frac{\partial\ell}{\partial\alpha}=0$, $\frac{\partial\ell}{\partial\beta}=0$, $\frac{\partial\ell}{\partial\lambda}=0$, and $\frac{\partial\ell}{\partial\xi}=0$ provides the following estimation system:

$$\frac{\partial\ell}{\partial\alpha} = \sum_{i=1}^{m}\frac{\delta_{i,1}}{\alpha+\beta y_{i:m}+\lambda y_{i:m}^2} + \sum_{i=1}^{m}\frac{\delta_{i,2}}{\alpha+\beta\,\psi(y_{i:m})+\lambda\,(\psi(y_{i:m}))^2} - \sum_{i=1}^{m}(r_i+1)\left[\delta_{i,1}\,y_{i:m}-\delta_{i,2}\,\psi(y_{i:m})\right]=0, \tag{3.2}$$

$$\frac{\partial \ell}{\partial \beta} = \sum_{i=1}^{m} \frac{\delta_{i,1}\, y_{i:m}}{\alpha + \beta y_{i:m} + \lambda y_{i:m}^2} + \sum_{i=1}^{m} \frac{\delta_{i,2}\, \psi(y_{i:m})}{\alpha + \beta\, \psi(y_{i:m}) + \lambda\, (\psi(y_{i:m}))^2} - \frac{1}{2} \sum_{i=1}^{m} (r_i + 1) \left[\delta_{i,1}\, y_{i:m}^2 + \delta_{i,2}\, (\psi(y_{i:m}))^2\right] = 0, \tag{3.3}$$

$$\frac{\partial \ell}{\partial \lambda} = \sum_{i=1}^{m} \frac{\delta_{i,1}\, y_{i:m}^2}{\alpha + \beta y_{i:m} + \lambda y_{i:m}^2} + \sum_{i=1}^{m} \frac{\delta_{i,2}\, (\psi(y_{i:m}))^2}{\alpha + \beta\, \psi(y_{i:m}) + \lambda\, (\psi(y_{i:m}))^2} - \frac{1}{3} \sum_{i=1}^{m} (r_i + 1) \left[\delta_{i,1}\, y_{i:m}^3 + \delta_{i,2}\, (\psi(y_{i:m}))^3\right] = 0, \tag{3.4}$$

$$\frac{\partial \ell}{\partial \xi} = \frac{n_2}{\xi} + \sum_{i=1}^{m} \frac{\delta_{i,2}\, (y_{i:m} - \tau)\, [\beta + 2\, \lambda\, \psi(y_{i:m})]}{\alpha + \beta\, \psi(y_{i:m}) + \lambda\, (\psi(y_{i:m}))^2} - \sum_{i=1}^{m} \delta_{i,2}\, (r_i + 1)\, (y_{i:m} - \tau) \left[\alpha + \beta\, \psi(y_{i:m}) + \lambda\, (\psi(y_{i:m}))^2\right] = 0. \tag{3.5}$$

Since closed-form solutions are impossible, instead, we will simply use the Newton-Raphson method outlined by El-Sagheer et al. [17] to compute the solution to the equation with Wolfram Mathematica software 13.1. The ML method is favored for its asymptotic unbiasedness, consistency, efficiency, normality, minimum-variance, and invariance properties as outlined by Azzalini [39], Eliason [40], and Held and Sabanés Bové [41]. Invariance ensures that estimates of $R(t)$ and $h(t)$ can be obtained by substituting $\hat{\Theta}$ into Eqs (2.6) and (2.7).

3.2. Bayesian estimation via MCMC

In the Bayesian approach, the unknown parameters are considered to be random variables. Before any failure data are seen, a joint prior distribution is specified to reflect prior knowledge, a situation where a prior distribution is especially useful because of low sample sizes. To derive Bayesian estimates (BEs) for the QHRD parameters in addition to the AF, SF, and HF, we make use of independent informative priors.

$$\alpha \sim \text{Gamma}(\mu_1, \nu_1), \quad \beta \sim \mathcal{N}(\mu_2, \nu_2^2), \quad \lambda \sim \text{Gamma}(\mu_3, \nu_3), \quad \xi \sim \text{Gamma}(\mu_4, \nu_4),$$

where all hyperparameters satisfy $\mu_i, \nu_i > 0$ for $i = 1, 3, 4$, and $\nu_2^2 > 0$ (with $\mu_2 \in \mathbb{R}$). Their densities are

$$\left.\begin{aligned} &\pi_1(\alpha) = \frac{\nu_1^{\mu_1}}{\Gamma(\mu_1)} \alpha^{\mu_1 - 1} e^{-\nu_1 \alpha}, \alpha \geq 0, \mu_1, \nu_1 > 0,\ \pi_2(\beta) = \frac{1}{\sqrt{2\pi\nu_2^2}} e^{-\frac{(\beta - \mu_2)^2}{2\nu_2^2}}, \beta \geq -2\sqrt{\alpha\lambda},\ \mu_2 \in \mathbb{R},\ \nu_2^2 > 0, \\ &\pi_3(\lambda) = \frac{\nu_3^{\mu_3}}{\Gamma(\mu_3)} \lambda^{\mu_3 - 1} e^{-\nu_3 \lambda}, \lambda \geq 0, \mu_3, \nu_3 > 0,\ \pi_4(\xi) = \frac{\nu_4^{\mu_4}}{\Gamma(\mu_4)} \xi^{\mu_4 - 1} e^{-\nu_4 \xi}, \xi > 1, \mu_4, \nu_4 > 0. \end{aligned}\right\}. \tag{3.6}$$

Hence, the joint prior is

$$\pi(\Theta) \propto \alpha^{\mu_1 - 1} \lambda^{\mu_3 - 1} \xi^{\mu_4 - 1} e^{-\left(\nu_1 \alpha + \frac{(\beta - \mu_2)^2}{2\nu_2^2} + \nu_3 \lambda + \nu_4 \xi\right)},\ \text{where } \mu_1, \mu_3, \mu_4, \nu_1, \nu_3, \nu_4 > 0, \mu_2 \in \mathbb{R},\ \text{and } \nu_2^2 > 0. \tag{3.7}$$

Combining the likelihood $\mathcal{L}$ from Eq (3.1) with Eq (3.7) yields the un-normalized joint posterior $\pi^*(\Theta \mid data) \propto \mathcal{L}(\Theta)\, \pi(\Theta)$ with the normalizing constant $\mathcal{A} = \int_0^\infty \int_0^\infty \int_0^\infty \int_{-2\sqrt{\alpha\lambda}}^\infty \mathcal{L}(\Theta)\, \pi(\Theta)\, d\beta\, d\alpha\, d\lambda\, d\xi$.

Explicitly, one obtains

$$\begin{aligned}\pi^*(\Theta \mid \text{data}) \propto\ & \alpha^{\mu_1-1}\,\lambda^{\mu_3-1}\,\xi^{\mu_4-1}\,e^{-\left(\nu_1\alpha+\frac{(\beta-\mu_2)^2}{2\nu_2^2}+\nu_3\lambda+\nu_4\xi\right)} \\ & \times\prod_{i=1}^{m}\left\{\left(\alpha+\beta y_{i:m}+\lambda y_{i:m}^2\right)^{\delta_{i,1}} e^{-\delta_{i,1}(r_i+1)\left(\alpha y_{i:m}+\frac{\beta}{2}y_{i:m}^2+\frac{\lambda}{3}y_{i:m}^3\right)}\right\} \\ & \times\left\{\xi^{\delta_{i,2}}\left[\alpha+\beta\,\psi(y_{i:m})+\lambda\,(\psi(y_{i:m}))^2\right]^{\delta_{i,2}} e^{-\delta_{i,2}(r_i+1)\left[\alpha\,\psi(y_{i:m})+\frac{\beta}{2}(\psi(y_{i:m}))^2+\frac{\lambda}{3}(\psi(y_{i:m}))^3\right]}\right\}.\end{aligned} \tag{3.8}$$

The conditional posteriors $\pi_1^*(\alpha \mid \cdot) = \pi_1^*(\alpha \mid \beta, \lambda, \xi, data)$, $\pi_2^*(\beta \mid \cdot) = \pi_2^*(\beta \mid \alpha, \lambda, \xi, data)$, $\pi_3^*(\lambda \mid \cdot) = \pi_3^*(\lambda \mid \alpha, \beta, \xi, data)$, and $\pi_4^*(\xi \mid \cdot) = \pi_4^*(\xi \mid \alpha, \beta, \lambda, data)$ for each component are then

$$\begin{aligned}\pi_1^*(\alpha \mid \cdot) \propto\ & \alpha^{\mu_1-1}\,e^{-\alpha\left\{\nu_1+\sum_{i=1}^{m}(r_i+1)\left[\delta_{i,1}\,y_{i:m}-\delta_{i,2}\,\psi(y_{i:m})\right]\right\}} \\ & \times\prod_{i=1}^{m}\left\{\left(\alpha+\beta y_{i:m}+\lambda y_{i:m}^2\right)^{\delta_{i,1}}\left[\alpha+\beta\,\psi(y_{i:m})+\lambda\,(\psi(y_{i:m}))^2\right]^{\delta_{i,2}}\right\},\end{aligned} \tag{3.9}$$

$$\begin{aligned}\pi_2^*(\beta \mid \cdot) \propto\ & e^{-\left\{\frac{(\beta-\mu_2)^2}{2\nu_2^2}+\frac{\beta}{2}\sum_{i=1}^{m}(r_i+1)\left[\delta_{i,1}\,y_{i:m}^2+\delta_{i,2}(\psi(y_{i:m}))^2\right]\right\}} \\ & \times\prod_{i=1}^{m}\left\{\left(\alpha+\beta y_{i:m}+\lambda y_{i:m}^2\right)^{\delta_{i,1}}\left[\alpha+\beta\,\psi(y_{i:m})+\lambda\,(\psi(y_{i:m}))^2\right]^{\delta_{i,2}}\right\},\end{aligned} \tag{3.10}$$

$$\begin{aligned}\pi_3^*(\lambda \mid \cdot) \propto\ & \lambda^{\mu_3-1}\,e^{-\frac{\lambda}{3}\left\{3\nu_3+\sum_{i=1}^{m}(r_i+1)\left[\delta_{i,1}\,y_{i:m}^3+\delta_{i,3}(\psi(y_{i:m}))^2\right]\right\}} \\ & \times\prod_{i=1}^{m}\left\{\left(\alpha+\beta y_{i:m}+\lambda y_{i:m}^2\right)^{\delta_{i,1}}\left[\alpha+\beta\,\psi(y_{i:m})+\lambda\,(\psi(y_{i:m}))^2\right]^{\delta_{i,2}}\right\},\end{aligned} \tag{3.11}$$

$$\pi_4^*(\xi \mid \cdot) \propto \xi^{\mu_4+n_2-1}\,e^{-\left\{\nu_4\xi+\sum_{i=1}^{m}\delta_{i,2}(r_i+1)\left[\alpha\,\psi(y_{i:m})+\frac{\beta}{2}(\psi(y_{i:m}))^2+\frac{\lambda}{3}(\psi(y_{i:m}))^3\right]\right\}}\prod_{i=1}^{m}\left[\alpha+\beta\,\psi(y_{i:m})+\lambda\,(\psi(y_{i:m}))^2\right]^{\delta_{i,2}}. \tag{3.12}$$

Closed-form BEs under three different loss functions, namely, the symmetric squared-error loss function (SELF), the asymmetric linear exponential loss function (LINEXLF) proposed by Zellner [42], and the asymmetric general entropy loss (GELF) introduced by Calabria and Pulcini [43], when the expression is a general function $g(\Theta)$, are stated in terms of the posterior mean as follows:

$$\hat{g}_{SEL}(\Theta) = E\left[g(\Theta) \mid data\right] = \int_0^\infty\int_0^\infty\int_0^\infty\int_{-2\sqrt{\alpha\lambda}}^\infty g(\Theta)\,\pi^*(\Theta \mid data)\,d\beta\,d\alpha\,d\lambda\,d\xi. \tag{3.13}$$

$$\hat{g}_{LINEX}(\Theta) = \frac{-1}{c}\ln\left|E\left[e^{-cg(\Theta)} \mid data\right]\right| = \frac{-1}{c}\ln\left|\int_0^\infty\int_0^\infty\int_0^\infty\int_{-2\sqrt{\alpha\lambda}}^\infty e^{-c\,g(\Theta)}\,\pi^*(\Theta \mid data)\,d\beta\,d\alpha\,d\lambda\,d\xi\right|,\ c \neq 0. \tag{3.14}$$

$$\hat{g}_{GEL}(\Theta) = \{E\left[g(\Theta)^{-q} \mid data\right]\}^{\frac{-1}{q}} = \left\{\int_0^\infty \int_0^\infty \int_0^\infty \int_{-2\sqrt{\alpha\lambda}}^\infty g(\Theta)^{-q}\, \pi^*(\Theta \mid data)\, d\beta\, d\alpha\, d\lambda\, d\xi\right\}^{\frac{-1}{q}}, \quad q \neq 0. \tag{3.15}$$

Because the integrals in Eqs (3.13)–(3.15) are intractable, we resort to MCMC. Although Gibbs sampling naturally leverages the conditionals in Eqs (3.9)–(3.12), these are nonstandard. We therefore embed Metropolis-Hastings (M-H) steps with Gaussian proposals into each update, ensuring detailed balance and convergence to the target posterior; see Lynch [44]. A graphical depiction of the four conditional densities is shown in Figure 4.

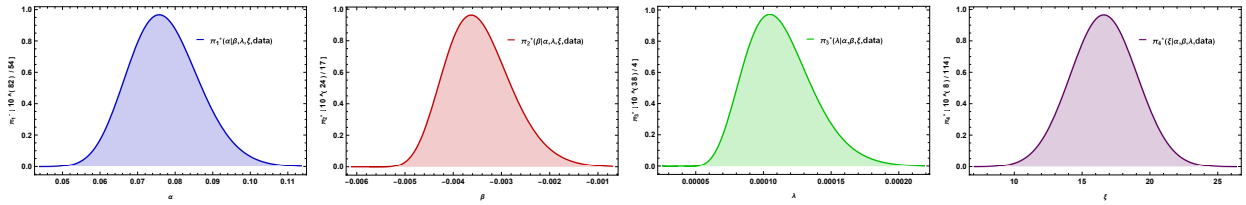

Figure 4. Conditional posterior densities for α (blue), β (red), λ (green), and ξ (purple).

3.2.1. Metropolis-Hastings within the Gibbs sampler

Building on the approach of Tierney [45] and the detailed exposition by Gilks et al. [46], we embed the M-H step into each cycle of a Gibbs sampler. The algorithm proceeds as follows:

(1) Initialization. For each parameter index $i = 1, 2, 3, 4$, set $\theta_i^{(0)} = \hat{\theta}_i$.
(2) Iteration counter. Let $j = 1$.
(3) Proposal generation. For each $i = 1, 2, 3, 4$, denote the full conditional target density as $\pi_i^*(\theta_i^{(j-1)} \mid \Theta_{-i}^{(j-1)}, \text{data})$, where $\Theta_{-i}^{(j-1)}$ denotes the other three components at the appropriate updated or previous values. At iteration j, draw a candidate θ_i^* from $\mathcal{N}\left(\theta_i^{(j-1)}, \hat{\sigma}^2_{\hat{\theta}_i}\right)$, where $\hat{\sigma}^2_{\hat{\theta}_i}$ is the ith diagonal element of the inverse Fisher information matrix (IFIM) (see Subsection 4.1).
(4) Acceptance test. For each $i = 1, 2, 3, 4$, compute $\eta_{\theta_i} = \min\left\{1, \frac{\pi_i^*(\theta_i^*|\Theta_{-i}^{(j-1)}, \text{data})}{\pi_i^*(\theta_i^{(j-1)}|\Theta_{-i}^{(j-1)}, \text{data})}\right\}$, generate $u_i \sim U(0, 1)$, and set $\theta_i^{(j)} = \begin{cases} \theta_i^*, & u_i < \eta_{\theta_i}, \\ \theta_i^{(j-1)}, & \text{otherwise.} \end{cases}$
(5) Compute the derived quantities. Update the reliability and hazard at iteration j by substituting $\theta_i^{(j)}$ into Eqs (2.6) and (2.7), thereby obtaining $R^{(j)}(t) = \theta_5^{(j)}$ and $h^{(j)}(t) = \theta_6^{(j)}$.
(6) Increment. Set $j \to j + 1$.
(7) Repeat. Perform Steps 3–6 for $j = 1, 2, \ldots, \mathcal{N}$.

Discard the first $\mathcal{M}$ draws as a burn-in period to reduce dependence on the initial values. For a sufficiently large total sample size $\mathcal{N}$, the remaining draws $\{\theta_i^{(j)} : j = \mathcal{M} + 1, \mathcal{M} + 2, \ldots, \mathcal{N}\}$ for $i = 1, 2, \ldots, 6$ serve as approximate posterior samples. Let $\mathcal{N}_{\mathcal{B}} = \mathcal{N} - \mathcal{M}$; then the BEs under different loss functions given in Eqs (3.13)–(3.15) are calculated by

$$\hat{\theta}_{i_{SEL}} = \frac{1}{\mathcal{N}_{\mathcal{B}}} \sum_{j=\mathcal{M}+1}^{\mathcal{N}} \theta_i^{(j)}, \quad \hat{\theta}_{i_{LINEX}} = \frac{-1}{c} \ln \left| \frac{1}{\mathcal{N}_{\mathcal{B}}} \sum_{j=\mathcal{M}+1}^{\mathcal{N}} e^{-c\,\theta_i^{(j)}} \right|, \quad \text{and} \quad \hat{\theta}_{i_{GEL}} = \left\{ \frac{1}{\mathcal{N}_{\mathcal{B}}} \sum_{j=\mathcal{M}+1}^{\mathcal{N}} (\theta_i^{(j)})^{-q} \right\}^{\frac{-1}{q}}.$$

3.2.2. Selection of hyperparameters

In Bayesian inference with informative priors, the specification of suitable hyperparameters is crucial and inevitable. This undertaking is usually achieved by a combination of expert judgment, already existing literature, and empirical evidence with the intention of exemplifying pertinent prior beliefs, which contributes to the increase in the robustness and interpretability of the models, as confirmed by Jaheen [47], Dey et al. [48], and Singh and Tripathi [49].

Let $\mathcal{W}$ be the number of complete datasets simulated from the QHRD under SSPALT. For each replicate $i = 1, 2, \ldots, \mathcal{W}$, denote the MLEs as $\hat{\Theta}_i = (\hat{\alpha}_i, \hat{\beta}_i, \hat{\lambda}_i, \hat{\xi}_i)$. We compute empirical moments as follows:

$$\overline{\theta}_k = \frac{1}{\mathcal{W}} \sum_{i=1}^{\mathcal{W}} \hat{\theta}_{k,i}, \quad \text{and} \quad \sigma^2_{\theta_k} = \frac{1}{\mathcal{W}-1} \sum_{i=1}^{\mathcal{W}} \left(\hat{\theta}_{k,i} - \overline{\theta}_k\right)^2, \quad \text{for} \quad k = 1, 2, 3, 4.$$

These are matched to the theoretical moments of the priors in Eq (3.6), namely:

$$\overline{\theta}_k = \begin{cases} \frac{\mu_k}{\nu_k}, & \text{for } k = 1, 3, 4, \\ \mu_k, & \text{for } k = 2, \end{cases} \quad \text{and} \quad \sigma^2_{\theta_k} = \begin{cases} \frac{\mu_k}{\nu_k^2}, & \text{for } k = 1, 3, 4, \\ \nu_k^2, & \text{for } k = 2. \end{cases}$$

Solving these equalities the following closed-form estimators:

$$\hat{\mu}_k = \begin{cases} \frac{\overline{\theta}_k^2}{\sigma^2_{\theta_k}}, & \text{for } k = 1, 3, 4, \\ \overline{\theta}_k^2, & \text{for } k = 2, \end{cases} \quad \text{and} \quad \hat{\nu}_k = \begin{cases} \frac{\overline{\theta}_k}{\sigma^2_{\theta_k}}, & \text{for } k = 1, 3, 4, \\ \sigma_{\theta_k}, & \text{for } k = 2. \end{cases}$$

This moment-matching strategy anchors our priors to the observed MLE variability, ensuring coherence between data-driven estimates and prior specifications.

4. Interval estimation under SSPALT with the P-T-II CS

In statistical inference, interval estimation provides a quantifiable range of plausible values for unknown model parameters. Frequentist confidence intervals (CIs) capture the variability inherent in repeated sampling and, at a prescribed confidence level, delimit a region that, under regularity, will contain the true parameter with the stated long-run frequency. As sample size grows, the precision of these intervals improves owing to their asymptotic properties. By contrast, Bayesian credible intervals (CRIs) are derived directly from the posterior distribution, melding prior information with observed data to yield a probability statement about where the parameter lies. Unlike CIs, which do not allow one to say that there is a 95% probability that the parameter lies in this interval, CRIs admit such a probabilistic interpretation. For a detailed treatment of CI methods, refer to the work of Lohr [50].

4.1. Asymptotic confidence intervals

Under standard regularity conditions, the MLEs $\hat{\Theta} = (\hat{\alpha}, \hat{\beta}, \hat{\lambda}, \hat{\xi})$ are asymptotically normal: $\hat{\Theta} \sim N\left(\Theta,\ \mathcal{I}(\Theta)^{-1}\right)$, where the Fisher information matrix (FIM) has the entries

$$\mathcal{I}_{ij}(\Theta) = E\left[-\frac{\partial^2 \ell(\Theta)}{\partial\theta_i \partial\theta_j}\right], \quad \text{for} \quad i, j = 1, 2, 3, 4.$$

Because these expectations are typically intractable, we substitute the observed information

$$\hat{\mathcal{I}}_{ij}(\Theta) = \left[-\frac{\partial^2 \ell(\Theta)}{\partial\theta_i \partial\theta_j}\right]_{\Theta=\hat{\Theta}}, \quad \text{for} \quad i, j = 1, 2, 3, 4.$$

and form its inverse

$$\hat{\mathcal{F}}\left(\hat{\Theta}\right) = \hat{\mathcal{I}}^{-1}\left(\hat{\Theta}\right) = \begin{pmatrix} -\frac{\partial^2 \ell}{\partial\alpha^2} & -\frac{\partial^2 \ell}{\partial\alpha\partial\beta} & -\frac{\partial^2 \ell}{\partial\alpha\partial\lambda} & -\frac{\partial^2 \ell}{\partial\alpha\partial\xi} \\ -\frac{\partial^2 \ell}{\partial\beta\partial\alpha} & -\frac{\partial^2 \ell}{\partial\beta^2} & -\frac{\partial^2 \ell}{\partial\beta\partial\lambda} & -\frac{\partial^2 \ell}{\partial\beta\partial\xi} \\ -\frac{\partial^2 \ell}{\partial\lambda\partial\alpha} & -\frac{\partial^2 \ell}{\partial\lambda\partial\beta} & -\frac{\partial^2 \ell}{\partial\lambda^2} & -\frac{\partial^2 \ell}{\partial\lambda\partial\xi} \\ -\frac{\partial^2 \ell}{\partial\xi\partial\alpha} & -\frac{\partial^2 \ell}{\partial\xi\partial\beta} & -\frac{\partial^2 \ell}{\partial\xi\partial\lambda} & -\frac{\partial^2 \ell}{\partial\xi^2} \end{pmatrix}^{-1}_{\Theta=\hat{\Theta}} = \begin{pmatrix} \hat{\sigma}^2_{\hat{\alpha}} & \hat{\sigma}_{\hat{\alpha}\hat{\beta}} & \hat{\sigma}_{\hat{\alpha}\hat{\lambda}} & \hat{\sigma}_{\hat{\alpha}\hat{\xi}} \\ \hat{\sigma}_{\hat{\alpha}\hat{\beta}} & \hat{\sigma}^2_{\hat{\beta}} & \hat{\sigma}_{\hat{\beta}\hat{\lambda}} & \hat{\sigma}_{\hat{\beta}\hat{\xi}} \\ \hat{\sigma}_{\hat{\alpha}\hat{\lambda}} & \hat{\sigma}_{\hat{\beta}\hat{\lambda}} & \hat{\sigma}^2_{\hat{\lambda}} & \hat{\sigma}_{\hat{\lambda}\hat{\xi}} \\ \hat{\sigma}_{\hat{\alpha}\hat{\xi}} & \hat{\sigma}_{\hat{\beta}\hat{\xi}} & \hat{\sigma}_{\hat{\lambda}\hat{\xi}} & \hat{\sigma}^2_{\hat{\xi}} \end{pmatrix}.$$

Thus, for each component $\hat{\theta}_i$ of $\hat{\Theta}$, a two-sided $100(1-\gamma)\%$ ACI is

$$\left(\hat{\theta}_{i_L}, \hat{\theta}_{i_U}\right) = \left(\hat{\theta}_i - z_{\gamma/2}\,\hat{\sigma}_{\hat{\theta}_i},\ \hat{\theta}_i + z_{\gamma/2}\,\hat{\sigma}_{\hat{\theta}_i}\right), \quad \text{for} \quad i = 1, 2, 3, 4,$$

where $z_{\gamma/2}$ is the upper $\gamma/2$ quantile of the standard normal distribution. In an attempt to obtain ACIs for $R(t)$ and $h(t)$, the delta method described by Greene [51] is used to estimate their variances. Let

$$\nabla\hat{R}(t) = \left(\partial_\alpha\hat{R}(t), \partial_\beta\hat{R}(t), \partial_\lambda\hat{R}(t), \partial_\xi\hat{R}(t)\right) \quad \text{and} \quad \nabla\hat{h}(t) = \left(\partial_\alpha\hat{h}(t), \partial_\beta\hat{h}(t), \partial_\lambda\hat{h}(t), \partial_\xi\hat{h}(t)\right).$$

Then $\hat{\sigma}^2_{\hat{R}(t)} = \nabla\hat{R}(t)^T\ \hat{\mathcal{F}}(\hat{\Theta})\ \nabla\hat{R}(t)$ and $\hat{\sigma}^2_{\hat{h}(t)}\nabla\hat{h}(t)^T\ \hat{\mathcal{F}}(\hat{\Theta})\ \nabla\hat{h}(t)$. Hence, the two-sided $100(1-\gamma)\%$ ACIs for $R(t)$ and $h(t)$ are

$$\left(\hat{R}(t)_L, \hat{R}(t)_U\right) = \left(\hat{R}(t) - z_{\gamma/2}\hat{\sigma}_{\hat{R}(t)}, \hat{R}(t) + z_{\gamma/2}\hat{\sigma}_{\hat{R}(t)}\right) \text{ and } \left(\hat{h}(t)_L, \hat{h}(t)_U\right) = \left(\hat{h}(t) - z_{\gamma/2}\hat{\sigma}_{\hat{h}(t)}, \hat{h}(t) + z_{\gamma/2}\hat{\sigma}_{\hat{h}(t)}\right).$$

4.2. Highest posterior density credible intervals

The HPD CRIs for each parameter θ_i are computed via the M-H steps within the Gibbs sampler described in Subsection 3.2. Denote the post-burn-in draws as $\theta_i^{(\mathcal{M}+1)} \le \theta_i^{(\mathcal{M}+2)} \le \cdots \le \theta_i^{(\mathcal{N})}$ for $i = 1, 2, \ldots, 6$.

A two-sided $100(1-\gamma)\%$ HPD interval is the shortest interval covering $(1-\gamma)$ of these sorted samples. Concretely, find the index j^* minimizing $\theta_i^{(j+\lfloor(1-\gamma)(\mathcal{N}-\mathcal{M})\rfloor)} - \theta_i^{(j)}$, $j = 1, 2, \ldots, \gamma(\mathcal{N}-\mathcal{M})$, where $\lfloor\chi\rfloor$ represents the largest integer $\le \chi$, and set $(\theta_{i_L}, \theta_{i_U}) = \left(\theta_i^{(j^*)}, \theta_i^{(j^*+\lfloor(1-\gamma)(\mathcal{N}-\mathcal{M})\rfloor)}\right)$.

5. Real engineering applications

In this section, we demonstrate how the QHRD can be applied practically and effectively to SSPALT, using the P-T-II CS and illustrating that with three real-world engineering applications.

- Solar lighting equipment (SLE) ($\tau = 5$; bi-level stress): When a SLE was tested at 293 K initially and then exposed to 353 K at $\tau = 5$, 16 failures were observed at first, while 15 failed after the thermal ramp-up, proving that more thermal stress leads to less reliability, an issue investigated before by Al-Essa et al. [52] and presented in Table 1.

Table 1. The SLE's data at normal (293) K and accelerated (353) K stress at ($\tau = 5$).

Normal stress (before $\tau = 5$)								Accelerated stress (after $\tau = 5$)							
0.140	0.783	1.324	1.582	1.716	1.794	1.883	2.293	5.002	5.022	5.082	5.112	5.147	5.238	5.244	5.247
2.660	2.674	2.725	3.085	3.924	4.396	4.612	4.892	5.305	5.337	5.407	5.408	5.445	5.483	5.717	

- Nanocrystalline embedded high-K (NCEH-k) devices ($\tau = 10$ min): Lifetime data (in minutes) of 40 NCEH-k devices analyzed under a single-step stress at $\tau = 10$ min yielded 38 failures, which were previously examined by Amleh and Raqab [53], and are presented in Table 2.

Table 2. NCEH-k devices' data at normal and accelerated stress at ($\tau = 10$ min).

Normal stress (before $\tau = 10$ min)								Accelerated stress (after $\tau = 10$ min)							
0.133	0.633	1.200	1.617	2.033	2.333	2.717	2.833	10.133	10.183	10.233	10.250	10.267	10.333	10.383	10.383
3.133	3.300	3.717	4.267	4.283	4.417	7.467		10.400	10.400	10.517	10.600	10.767	10.900	11.000	11.217
								11.250	11.333	11.400	11.533	11.550	12.167	12.417	

- Micro unmanned aerial vehicle (MUAV) ($\tau = 15$): Prototype MUAVs were subjected to wind-speed levels changing at $\tau = 15$, and the failure occurrences were tabulated to assess mission-critical power- systems' reliability under varying aerodynamic stress, which was previously investigated by Al-Essa et al. [52], and are presented in Table 3.

Table 3. MUAV's data at normal and accelerated stress at ($\tau = 15$).

Normal stress (before $\tau = 15$)								Accelerated stress (after $\tau = 15$)							
2.365	3.467	5.386	7.714	9.578	9.683	11.416	11.789	15.325	15.781	16.105	16.362	17.178	17.366	17.803	19.578
12.039	14.928	14.938													

The stress-change time τ is determined earlier, before experimentation, based on engineering constraints, pilot testing, or operational requirements. Through the three real applications presented, τ corresponds to physically meaningful stress-transition points defined by the experimental protocol described by Al-Essa et al. [52] and Amleh and Raqab [53]. The inferential framework developed herein is conditional on a fixed τ, which is standard practice in the accelerated testing literature described by Goel [34]. The proposed estimation procedures remain valid for any pre-specified τ. Initially, we obtain MLEs and corresponding standard errors (St.Ers) for both the QHRD and the AF. We then evaluate the fit of the QHRD to each of the three data-sets using the Cramér-von Mises statistic W^*, the Anderson-Darling statistic A^*, and the Kolmogorov-Smirnov test statistic D (with its associated P-value). In addition, we calculate several information criteria, namely the deviance (-2ℓ), the Akaike Information Criterion (AIC), the consistent AIC (CAIC), the Bayesian information criterion (BIC), and the Hannan-Quinn information criterion (HQIC). For comparison, the QHRD under the SSPALT framework was contrasted against several alternative lifetime models, namely the Gompertz distribution (GOD), generalization of the Rayleigh distribution (GRD), the two-parameters Sujatha distribution (TPSD), the Weibull distribution (WD), the two-parameters Mirra distribution (TPMD), the Lindley distribution (LD), the Janardan distribution (JD), the Gamma

distribution (GD), and the Ailamujia distribution (AD). The numerical outcomes of these goodness-of-fit tests and model-selection measures are summarized in Tables 4–6. In all cases, the QHRD produces *P*-values exceeding the conventional 0.05 threshold, thus confirming a satisfactory fit.

Table 4. Comparison of goodness-of-fit metrics for the QHRD model under SSPALT versus alternative approaches, applied to the SLE's data.

	MLE(St.Er)											
Model	$\hat{\alpha}$	$\hat{\beta}$	$\hat{\lambda}$	$\hat{\xi}$	-2ℓ	AIC	CAIC	BIC	HQIC	W^*	A^*	K-S (P-value)
QHRD	0.097(0.072)	0.008(0.042)	0.003(0.007)	11.149(5.934)	83.466	91.466	93.004	97.202	93.335	0.032	0.216	0.086(0.960)
GOD	0.198(0.146)	0.084(0.037)	⋯	10.207(5.625)	83.150	89.150	90.039	93.452	90.553	0.032	0.210	0.093(0.929)
LHRD	0.072(0.052)	0.029(0.024)	⋯	12.634(5.511)	83.911	89.911	90.800	94.213	91.313	0.039	0.254	0.100(0.887)
GRD	0.013(0.008)	−0.395(0.165)	⋯	13.635(5.496)	83.865	89.865	90.754	94.167	91.267	0.037	0.246	0.101(0.882)
TPSD	0.450(0.106)	2.533(4.083)	⋯	13.549(4.967)	84.772	90.772	91.661	95.074	92.175	0.045	0.294	0.108(0.824)
WD	1.410(0.295)	0.075(0.038)	⋯	14.786(6.681)	84.579	90.579	91.467	94.880	91.981	0.043	0.287	0.108(0.822)
TPMD	0.478(0.119)	0.948(1.475)	⋯	12.893(4.921)	84.951	90.951	91.840	95.253	92.354	0.048	0.307	0.108(0.821)
LD	0.296(0.049)	⋯	⋯	16.773(5.151)	84.947	88.947	89.375	91.815	89.882	0.040	0.274	0.109(0.820)
ED	0.139(0.035)	⋯	⋯	25.802(9.273)	87.032	91.032	91.460	93.900	91.966	0.056	0.421	0.109(0.817)
JD	0.440(0.888)	1.427(2.577)	⋯	16.074(5.863)	84.907	90.907	91.796	95.209	92.310	0.042	0.283	0.110(0.806)
GD	1.503(0.449)	0.245(0.109)	⋯	17.786(7.430)	85.313	91.313	92.202	95.615	92.715	0.041	0.292	0.112(0.793)
AD	0.178(0.029)	⋯	⋯	13.871(4.224)	86.289	90.289	90.718	93.157	91.224	0.061	0.438	0.118(0.738)
RD	⋯	0.062(0.016)	⋯	8.7760(2.475)	87.685	91.685	92.113	94.553	92.620	0.113	0.857	0.150(0.444)

Table 5. Comparison of goodness-of-fit metrics for the QHRD model under SSPALT versus alternative approaches, applied to NCEH-k devices' data.

	MLE(St.Er)											
Model	$\hat{\alpha}$	$\hat{\beta}$	$\hat{\lambda}$	$\hat{\xi}$	-2ℓ	AIC	CAIC	BIC	HQIC	W^*	A^*	K-S (P-value)
QHRD	0.073(0.026)	−0.004(0.005)	0.0002(0.0004)	14.223(9.832)	152.798	160.798	162.010	167.348	163.128	0.068	0.363	0.119(0.612)
ShGD	0.866(0.219)	0.046(0.024)	⋯	25.163(11.50)	155.493	161.493	162.199	166.406	163.241	0.118	0.625	0.139(0.413)
GD	0.861(0.224)	0.042(0.023)	⋯	25.320(11.57)	155.503	161.503	162.209	166.416	163.251	0.118	0.621	0.139(0.413)
GRD	0.001(0.001)	−0.641(0.088)	⋯	21.518(10.44)	153.808	159.808	160.514	164.721	161.556	0.084	0.470	0.142(0.387)
TPMD	0.108(0.038)	0.009(0.012)	⋯	19.771(7.501)	153.866	159.866	160.572	164.779	161.614	0.104	0.581	0.151(0.319)
TPSD	0.106(0.038)	234.6(304.5)	⋯	19.889(7.538)	153.982	159.982	160.688	164.895	161.730	0.106	0.595	0.152(0.311)
ED	0.055(0.014)	⋯	⋯	21.424(7.110)	155.841	159.841	160.183	163.116	161.006	0.136	0.750	0.154(0.299)
JD	0.002(0.005)	0.026(0.061)	⋯	20.228(7.462)	155.672	161.672	162.378	166.585	163.420	0.135	0.760	0.158(0.268)
LHRD	0.050(0.014)	0.001(0.001)	⋯	18.023(7.242)	155.149	161.149	161.855	166.062	162.897	0.133	0.770	0.165(0.227)
GOD	0.018(0.022)	0.049(0.013)	⋯	16.618(7.161)	154.808	160.808	161.514	165.721	162.556	0.130	0.772	0.168(0.208)

Table 6. Comparison of goodness-of-fit metrics for the QHRD model under SSPALT versus alternative approaches, applied to MUAV's data.

	MLE(St.Er)											
Model	$\hat{\alpha}$	$\hat{\beta}$	$\hat{\lambda}$	$\hat{\xi}$	-2ℓ	AIC	CAIC	BIC	HQIC	W^*	A^*	K-S (P-value)
GRD	0.003(0.002)	−0.030(0.343)	⋯	3.735(1.717)	108.855	114.855	116.455	117.688	115.334	0.018	0.134	0.081(0.999)
LHRD	3.6×10^{-7}(0.020)	0.007(0.004)	⋯	3.649(1.563)	108.862	114.862	116.462	117.695	115.342	0.018	0.141	0.082(0.998)
RD	⋯	0.007(0.002)	⋯	3.649(1.344)	108.862	112.862	113.612	114.751	113.182	0.018	0.141	0.082(0.998)
WD	2.038(0.540)	0.003(0.005)	⋯	3.551(1.868)	108.857	114.857	116.457	117.69	115.336	0.018	0.147	0.083(0.998)
TPSD	0.189(0.043)	2×10^{-5}(11.275)	⋯	4.532(1.959)	109.689	115.689	117.289	118.522	116.168	0.022	0.172	0.084(0.998)
QHRD	0.009(0.035)	0.003(0.012)	0.0003(0.0008)	2.926(1.705)	108.641	116.641	119.498	120.419	117.280	0.016	0.118	0.084(0.997)
GD	2.624(1.020)	0.167(0.088)	⋯	4.826(2.364)	109.717	115.717	117.317	118.550	116.197	0.022	0.164	0.090(0.994)
JD	605.76(52285.1)	5034.4(434532)	⋯	5.969(2.403)	110.176	116.176	117.776	119.009	116.655	0.025	0.157	0.110(0.957)
AD	0.060(0.012)	⋯	⋯	5.969(2.403)	110.176	114.176	114.926	116.065	114.495	0.025	0.157	0.120(0.957)
LD	0.112(0.022)	⋯	⋯	6.442(2.595)	110.775	114.775	115.525	116.663	115.094	0.028	0.185	0.116(0.934)
ED	0.049(0.015)	⋯	⋯	10.48(4.869)	114.814	118.814	119.564	120.703	119.134	0.087	0.558	0.166(0.616)

These results suggest that the QHRD is better than the alternative approaches that were tested. Notice that significant values are highlighted in bold. Thus, there is no reason to deny that the theoretical and empirical distributions may be the same. To make the assessment of the QHRD complete, the CDF data and fitted curves from both it and the other competing distributions were layered together for comparison. In addition, each distribution was analyzed through histograms and highlighting the fitted PDFs. To further examine how well the models fit the data, probability-probability (P-P) plots and quantile-quantile (Q-Q) plots were built and displayed in Figure 5. The statistical tests and graphs confirm on every occasion that the QHRD provides a better match for all three data sets compared with the competing models.

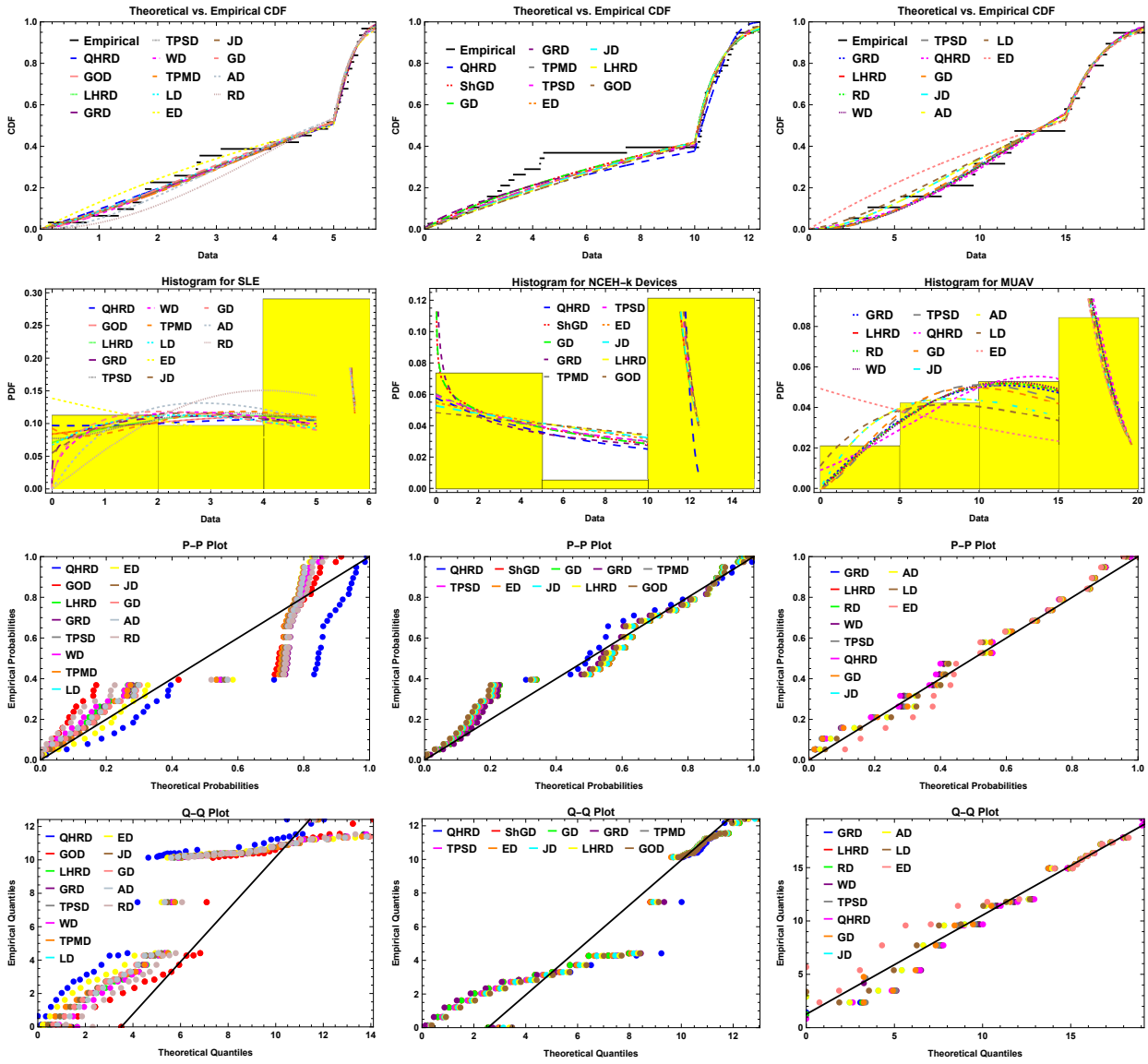

Figure 5. Comparison of empirical and fitted CDFs, histograms overlaid with fitted PDFs, P-P plots, and Q-Q plots for the SLE's data (left column), the NCEH-k devices' data (center column), and the MUAV's data (right column).

Now, according to the SSPALT framework with P-T-II CS with binomial removals, as described

in Section 1, where $p = 0.25$ and $m = 27$ for the SLE's data, $m = 22$ for the NCEH-k devices' data, and $m = 13$ for the MUAV's data. Accordingly, the corresponding censoring schemes $\mathbf{r}$ are as follows: For the SLE's data, it is $\mathbf{r} = (4^{(2)}, 0^{(4)}, 1, 0^{(15)})$; for the NCEH-k devices' data, it is $\mathbf{r} = (1, 2, 1, 3, 1, 0^{(3)}, 1, 0, 1^{(2)}, 0^{(15)})$; and for the MUAV's data, it is $\mathbf{r} = (5, 0^{(3)}, 1, 0^{(8)})$, along with their corresponding observed data presented in Tables 7–9.

Table 7. Observed data according to the SSPALT framework with the P-T-II CS from the SLE's data ($\tau = 5$).

Normal stress (before $\tau = 5$)								Accelerated stress (after $\tau = 5$)							
0.140	0.783	1.324	1.716	1.794	1.883	2.293	2.660	5.002	5.082	5.112	5.244	5.305	5.337	5.407	5.445
2.674	3.085	3.924	4.396	4.892				5.483							

Table 8. Observed data according to the SSPALT framework with the P-T-II CS from the NCEH-k devices' data ($\tau = 10$ min).

Normal stress (before $\tau = 10$ min)								Accelerated stress (after $\tau = 10$ min)							
0.133	0.633	1.200	1.617	2.033	2.717	2.833	3.133	10.133	10.183	10.250	10.267	10.383	10.400	10.517	10.600
3.300	3.717	4.267	4.417					10.767	11.000	11.250	11.533	11.550	12.167	12.417	

Table 9. Observed data according to the SSPALT framework with the P-T-II CS from the MUAV's data ($\tau = 15$).

Normal stress (before $\tau = 15$)								Accelerated stress (after $\tau = 15$)				
2.365	3.467	5.386	7.714	9.683	11.416	14.928	14.938	15.325	15.781	16.105	16.362	17.366

The point estimates and associated 95% ACIs, along with their standard errors (St.Er) and lower (L) and upper (U) bounds, for all datasets obtained via ML are summarized in Tables 10–12, together with the average lengths (ALs). In parallel, we ran 48,000 MCMC iterations, discarding the first 8,000 as burn-in to reduce the impact of the initial values. Following the procedure in Subsection 3.2.2, we generated $\mathcal{W} = 500$ independent random samples for each dataset. Each dataset contains $n = 100$ observations; therefore, the hyperparameters are defined in Table 13.

Table 10. Point and interval estimates for α, β, λ, ξ, $R(t)$, and $h(t)$ from the SLE's data.

	ML					Bayesian				
Par.	Est.	St.Er	L	U	AL	Est.	St.D	L	U	AL
α	0.10308	0.08738	−0.06818	0.27434	0.34252	0.09038	0.02182	0.04946	0.13379	0.08433
β	0.01041	0.05786	−0.10300	0.12383	0.22683	0.01682	0.00833	0.00007	0.03106	0.03099
λ	0.00450	0.00921	−0.01356	0.02255	0.03611	0.00259	0.00168	0.00003	0.00578	0.00574
ξ	10.0568	5.74132	−1.19602	21.3095	22.5055	11.8412	2.49913	7.29673	16.8007	9.50396
$R(5.2)$	0.22419	0.08738	0.07124	0.37715	0.30591	0.24139	0.05747	0.13379	0.35639	0.22260
$h(5.2)$	3.99365	0.05786	1.46761	6.51969	5.05208	4.08642	1.08067	2.10480	6.22868	4.12388

Table 11. Point and interval estimates for $\alpha, \beta, \lambda, \xi, R(t)$, and $h(t)$ from the NCEH-k devices' data.

	ML					Bayesian				
Par.	Est.	St.Er	L	U	AL	Est.	St.D	L	U	AL
α	0.076772	0.025899	0.026011	0.127533	0.101521	0.078370	0.013013	0.054112	0.104969	0.050858
β	−0.003601	0.003371	−0.010207	0.003005	0.013212	−0.004063	0.002355	−0.008404	−0.000019	0.008385
λ	0.000107	0.000154	−0.000194	0.000409	0.000603	0.000221	0.000179	1×10^{-6}	0.000561	0.000560
ξ	16.95760	10.14050	−2.917460	36.83270	39.75020	13.39470	3.951040	6.251460	21.19700	14.94560
$R(10.5)$	0.357146	0.025899	0.184792	0.529500	0.344707	0.357209	0.068341	0.230482	0.494598	0.264116
$h(10.5)$	0.795046	0.003371	0.246726	1.343370	1.096640	0.833361	0.217269	0.429374	1.275210	0.845839

Table 12. Point and interval estimates for $\alpha, \beta, \lambda, \xi, R(t)$, and $h(t)$ from the MUAV's data.

	ML					Bayesian				
Par.	Est.	St.Er	L	U	AL	Est.	St.D	L	U	AL
α	0.01817	0.03412	−0.04870	0.08505	0.13375	0.00968	0.00513	0.00138	0.01985	0.01847
β	0.00058	0.01045	−0.01989	0.02106	0.04095	0.00340	0.00142	0.00069	0.00619	0.00549
λ	0.00028	0.00066	−0.00101	0.00157	0.00258	0.00030	0.00014	0.00006	0.00057	0.00051
ξ	6.00020	3.83609	−1.51841	13.5188	15.0372	3.52504	0.64579	2.34254	4.82544	2.48289
$R(15.5)$	0.37843	0.03412	0.15763	0.59923	0.44160	0.34088	0.07722	0.19546	0.49317	0.29771
$h(15.5)$	0.72208	0.01045	0.15933	1.28483	1.12550	0.52482	0.15359	0.24772	0.82837	0.58064

Table 13. Values of the hyperparameters for each dataset.

Dataset	μ_1	ν_1	μ_2	ν_2	μ_3	ν_3	μ_4	ν_4
SLE	11.5926	135.091	0.0144	0.0107	1.5904	621.475	14.0265	1.1514
NCEH-k	22.6541	295.431	−0.0057	0.0043	0.6753	1970.11	6.6466	0.4425
MUAV	3.16786	325.210	0.0033	0.0018	2.6823	9566.00	22.9788	7.1755

The BEs, including their St.Er and 95% HPD CRIs with the corresponding L and U bounds and ALs, are likewise tabulated. A comparison of the interval widths shows that the HPD CRIs are uniformly narrower than the ACIs, thereby highlighting the enhanced precision afforded by the Bayesian framework.

The outcomes of the Bayesian inference given in Tables 10–12 generate some critical conclusions. According to the SLE dataset, 24% of the units are expected to survive at $t = 5.2$, which will be a critical failure point where the hazard rate would increase significantly to 4.09. This finding further underscores the need for improved thermal management and maintenance strategies. The NCEH-k devices were found to have a reliability of about 36% at $t = 10.5$, and the high hazard rate value of 0.83 indicates that the design should be reinforced after the relaxation of stress. Lastly, for the MUAV dataset, about 34% of the systems are projected to survive beyond $t = 15.5$, facing a 52.5% instantaneous failure risk, underlining the importance of improved design and operational protocols to mitigate failures after the stress transition. To enhance both the precision and robustness of the parameter estimates, we derive the profile log-likelihood functions and their first-order partial derivatives as given in (3.1)–(3.5). At the resulting MLEs, we also generate contour plots of the

log-likelihood surface. The profile log-likelihood curves and their derivatives are displayed in Figures 6–8, while the corresponding contour diagrams appear in Figures 9–11. The fact that each function reaches its global maximum at the MLEs confirms both the existence and uniqueness of these estimates.

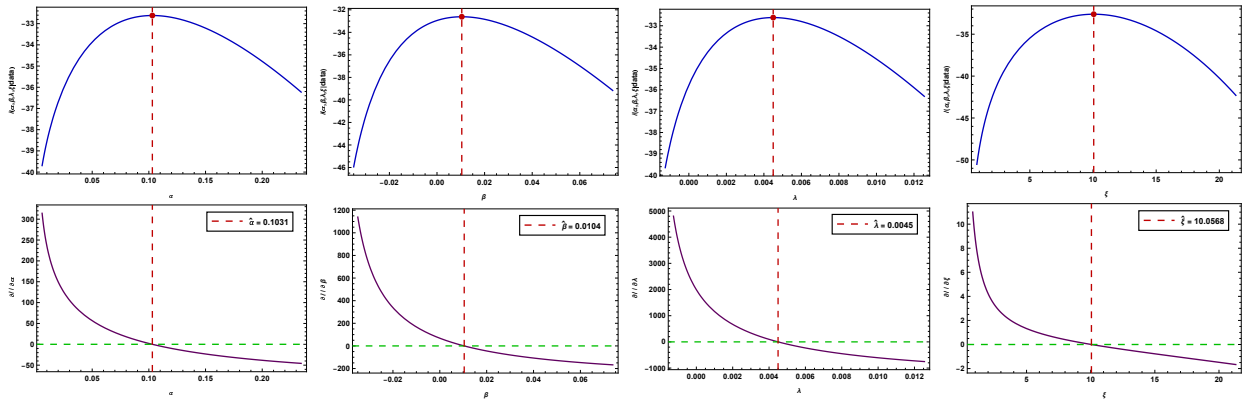

Figure 6. Profile log-likelihood (blue curves, upper) alongside their first partial derivatives (purple curves, lower), including the ML (big red point) for the parameters, based on the SLE's data.

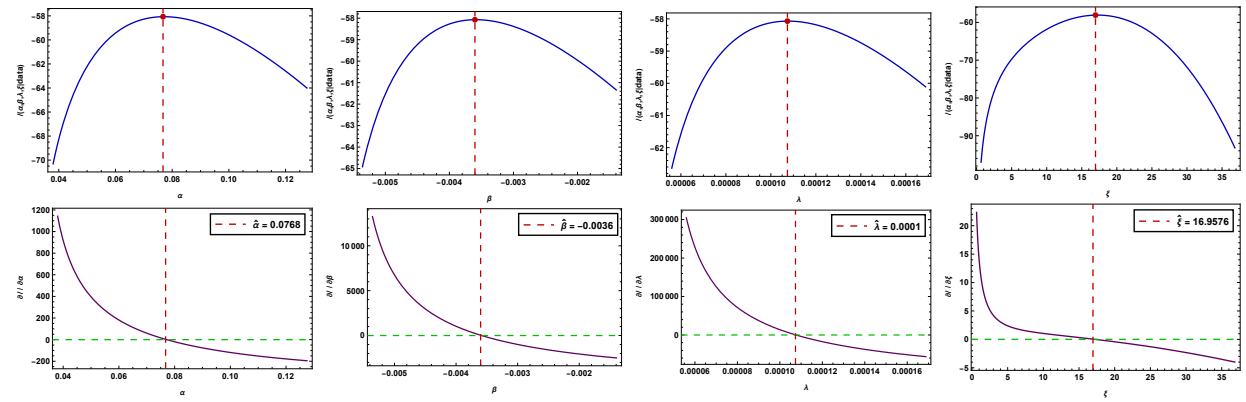

Figure 7. Profile log-likelihood (blue curves, upper) alongside their first partial derivatives (purple curves, lower), including the ML (big red point) for the parameters, based on the NCEH-k devices' data.

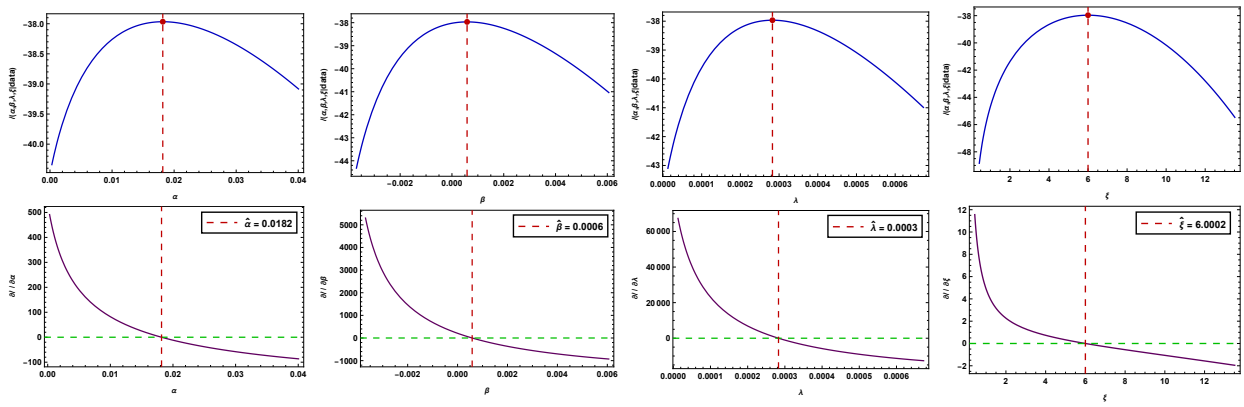

Figure 8. Profile log-likelihood (blue curves, upper) alongside their first partial derivatives (purple curves, lower), including the ML (big red point) for the parameters, based on the MUAV's data.

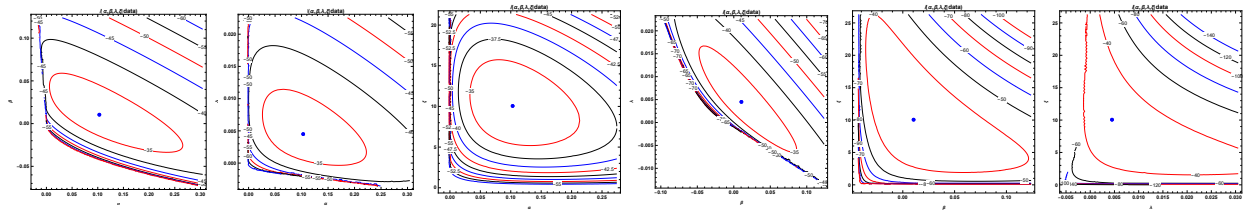

Figure 9. Contour curves of the log-likelihood surface with the global optimum indicated for the parameters, based on the SLE's data.

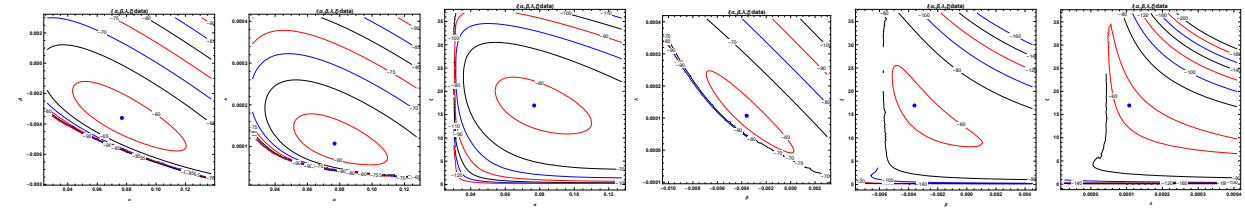

Figure 10. Contour curves of the log-likelihood surface with the global optimum indicated for the parameters, based on the NCEH-k devices' data.

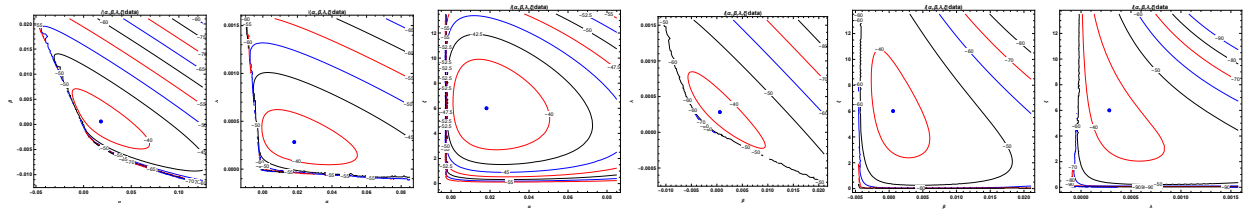

Figure 11. Contour curves of the log-likelihood surface with the global optimum indicated for the parameters, based on the MUAV's data.

To assess the convergence behavior of the MCMC chains, in Figures 12–14, we present the trace plots, their convergence, and their Gaussian kernel density estimates. Each figure displays histograms

for the parameters α, β, and λ, as well as for $R(t)$ and $h(t)$. A dashed blue line indicates the posterior mean, while solid blue lines mark the bounds of the 95% HPD CRIs. The stable, well-mixed traces and the near-symmetry of the density estimates together indicate satisfactory convergence and consistency among the posterior summaries. The numerical results summarized in Tables 10–12 also demonstrate that the BEs achieve the lowest St.Ers and the shortest ALs, confirming their superior performance in this context.

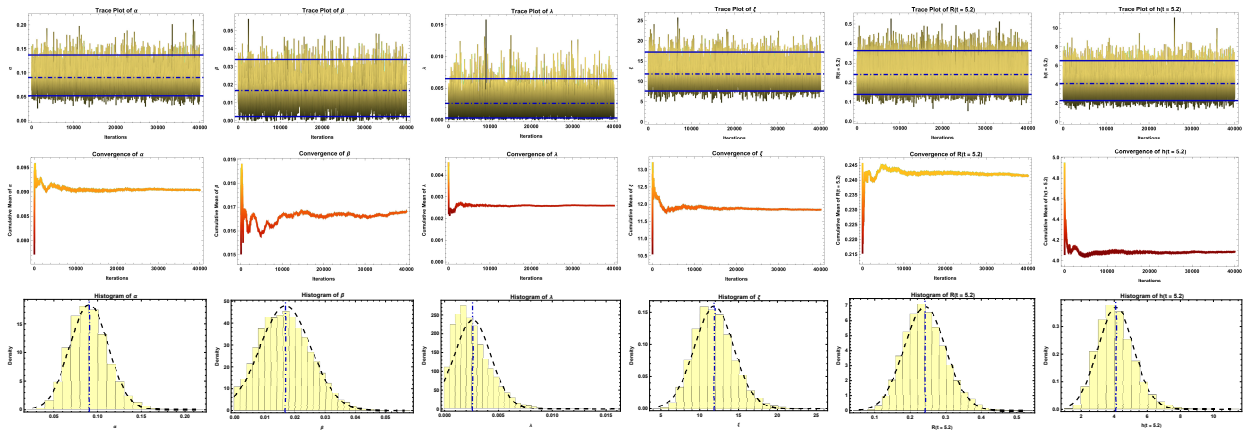

Figure 12. MCMC trace plots (top) and convergence (center) along with histograms and proposal distribution (normal) plots (bottom) for the MLEs of α, β, λ, ξ, $R(t)$, and $h(t)$ for the SLE's data.

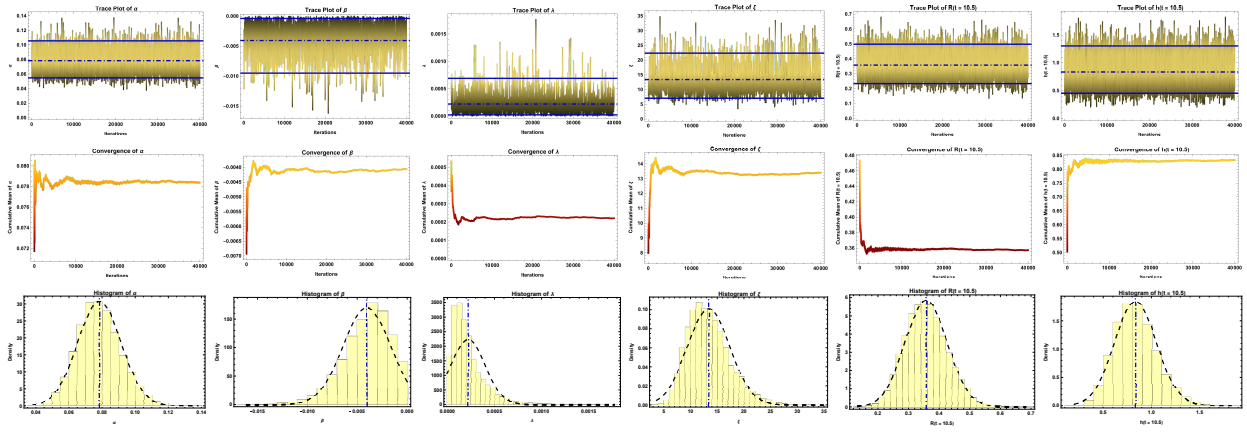

Figure 13. MCMC trace plots (top) and convergence (center) along with histograms and proposal distribution (normal) plots (bottom) for the MLEs of α, β, λ, ξ, $R(t)$, and $h(t)$ for the NCEH-k devices' data.

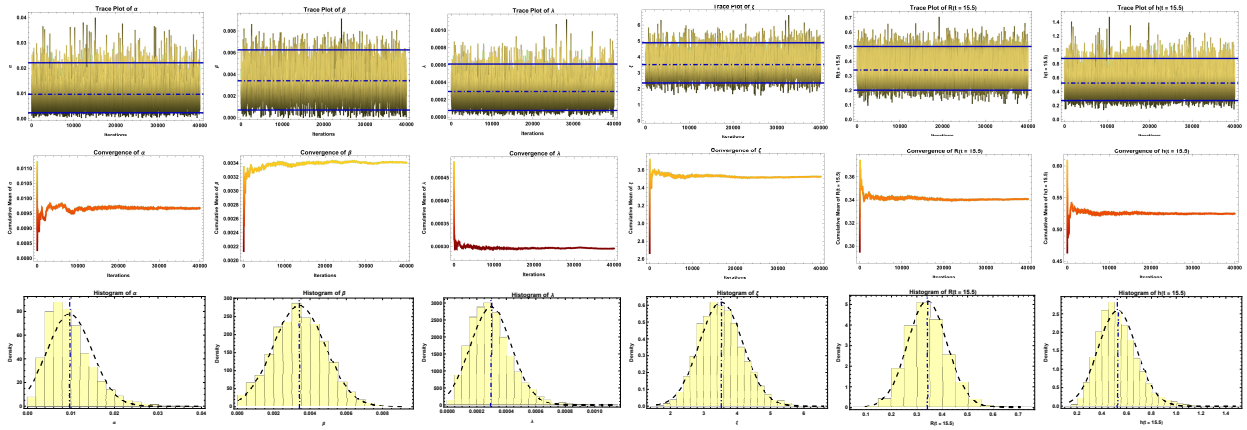

Figure 14. MCMC trace plots (top) and convergence (center) along with histograms and proposal distribution (normal) plots (bottom) for the MLEs of α, β, λ, ξ, $R(t)$, and $h(t)$ for the MUAV's data.

6. Simulation study

In this part, we carry out a Monte Carlo simulation to assess the validity and effectiveness of both the ML and Bayesian counterparts to the parameters of the QHRD and AF, as well as derived quantities, namely the RF and HF, in the context of SSPALT with P-T-II censored samples. Using Wolfram Mathematica software version 13.2, 1000 P-T-II samples were generated from the QHRD under SSPALT using binomial removals for every simulation run. The samples have been generated with a random set of initial values of the parameters, $\alpha_0 = 0.68$, $\beta_0 = -2.49$, $\lambda_0 = 3.76$, and $\xi_0 = 1.59$ at a time $t = 1.02$ and a stress change time $\tau = 1$. The $R(t = 1.02)$ and $h(t = 1.02)$ values were 0.471 and 3.361, respectively. We examine a number of values of the sample sizes (n) along with the censored sample sizes (m) and the removal probabilities (p) given in Table 14.

Table 14. Different censoring schemes proposed in the simulation study.

Scheme	S[1]	S[2]	S[3]	S[4]	S[5]	S[6]
(n, m, p)	$(80, 32, 0.2)$	$(80, 32, 0.4)$	$(80, 32, 0.6)$	$(80, 48, 0.2)$	$(80, 48, 0.4)$	$(80, 48, 0.6)$
Scheme	S[7]	S[8]	S[9]	S[10]	S[11]	S[12]
(n, m, p)	$(160, 64, 0.2)$	$(160, 64, 0.4)$	$(160, 64, 0.6)$	$(160, 96, 0.2)$	$(160, 96, 0.4)$	$(160, 96, 0.6)$

The estimation process is carried out in several main steps.

(1) Initialization. Specify (n, m, p, τ) and set the starting values $(\alpha_0, \beta_0, \lambda_0, \xi_0)$.
(2) Sample generation. Draw n complete lifetimes from the QHRD under SSPALT by sampling from the CDF $F(y)$ given in Eq (2.5), then apply the P-T-II CS described in Section 2.
(3) ML. Compute the MLEs $\hat{\Theta} = (\hat{\alpha}, \hat{\beta}, \hat{\lambda}, \hat{\xi})$ and the corresponding RF and HF at $t = 1.02$. Construct the associated 95% ACIs described in Subsection 4.1.
(4) Bayesian estimation. Adopt informative priors and define their hyperparameters as in Subsection 3.2.2 by generating $\mathcal{W} = 500$ complete random samples from the QHRD using the initial values of the parameters, each containing $n = 100$ observations. Therefore, the

hyperparameters are specified as follows: $\mu_1 = 9.58675, \nu_1 = 14.2014, \mu_2 = -2.44792, \nu_2 = 1.08033, \mu_3 = 9.21707, \nu_3 = 2.48062, \mu_4 = 26.4847$, and $\nu_4 = 15.8018$. Then run an MCMC sampler for $\mathcal{N} = 12000$ iterations, discarding the first $\mathcal{M} = 2000$ as burn-in. From the posterior draws, obtain the BEs and 95% HPD CRIs.

(5) Replication. Repeat Steps 1–4 for $\mathcal{B} = 1000$ Monte Carlo replications to ensure stable inference.

(6) Performance metrics. For each point estimate of θ_i, where $i = 1, 2, \ldots, 6$, compute the following:

$$\text{AEst}(\theta_i) = \frac{1}{\mathcal{B}}\sum_{j=1}^{\mathcal{B}}\hat{\theta}_i^{(j)}, \quad \text{RMSE}(\theta_i) = \sqrt{\frac{1}{\mathcal{B}}\sum_{j=1}^{\mathcal{B}}\left(\hat{\theta}_i^{(j)} - \theta_i\right)^2}, \quad \text{and} \quad \text{MRAB}(\theta_i) = \frac{1}{\mathcal{B}}\sum_{j=1}^{\mathcal{B}}\left|\frac{\hat{\theta}_i^{(j)} - \theta_i}{\theta_i}\right|.$$

Likewise, the interval estimation is assessed using the following measures:

$$\text{AL}_{(1-\gamma)\%}(\theta_i) = \frac{1}{\mathcal{B}}\sum_{j=1}^{\mathcal{B}}\left(\hat{\theta}_{i_U}^{(j)} - \hat{\theta}_{i_L}^{(j)}\right) \quad \text{and} \quad \text{CP}_{(1-\gamma)\%}(\theta_i) = \frac{1}{\mathcal{B}}\sum_{j=1}^{\mathcal{B}}\mathbf{1}_{[\hat{\theta}_{i_L}^{(j)}, \hat{\theta}_{i_U}^{(j)}]}(\theta_i).$$

Here, AEst represents the average estimate of a parameter across all simulation replications; RMSE represents the root mean square error and measures the precision of estimation of the parameter; MRAB represents the mean relative absolute bias, which refers to the average proportional difference between the estimate and the true parameter value; AL represents the average length of the constructed intervals (either ACI or HPD CRIs); and CP refers to the coverage probability, indicating the percentage of intervals that cover the true parameter value.

6.1. Simulation results

The findings are comprehensively presented in Tables 15–17 for each parameter under the SSPALT with the P-T-II CS, which include the AEst, RMSE, MRAB, AL, and CP of the 95% ACI or HPD CRIs. In these tables, ML is the MLEs, BS is the BEs based on the SELF, BL1 and BL2 are the BEs based on the LINEXLF with $c = -0.3$ and $c = 0.3$, and BG1 and BG2 are the BEs based on the GELF with $q = -1$ and $q = 1$. The findings provide significance for the behavior of the point and interval estimates, especially the desirable trends of a lower RMSE, MRAB, and AL and a maximum CP. Specifically, the following observations are noteworthy.

- General observations across parameters
  - Bayesian estimators (BS, BL1, BL2, BG1, BG2) consistently outperform the classical MLE in terms of lower RMSE and MRAB.
  - HPD CRIs have higher CPs (near or above 95%), and their ALs are substantially shorter than the ML ACIs.
  - Asymmetric loss functions (LINEXLF and GELF) effects on the direction of bias: Negative parameters overestimate, and positive parameters underestimate.
  - In aggregate, the Bayesian methods give more accurate and reliable point and interval estimates in SSPALT, given the P-T-II CS.
- Parameter-specific insights
  - α and β: BEs have a lower RMSE than ML by more than a half; the intervals are shorter and have better coverage.

  - λ and ξ: BEs dramatically improve precision and interval reliability; ML intervals tend to undercover and are much wider.
  - $R(t)$ and $h(t)$: BEs provide more accurate and stable estimates along with shorter credible intervals compared with ML.
- Effect of censoring schemes
  - The larger the sample size is, the more accurate the estimation and interval precision.
  - Increasing censoring (greater probability of removal) decreases performance in a relatively small way, worsening the RMSE and AL and decreasing coverage in some cases.
  - BEs remain robust across all censoring schemes, maintaining high coverage and efficiency.
- Overall, the MCMC framework with suitable loss functions provides a suitable tradeoff of competence, dependability, and interpretability to practitioners who study progressively censored data.

Table 15. Results of point and interval estimates for α and β under SSPALT with the P-T-II CS.

Scheme		α						β					
		ML	BS	BL1	BL2	BG1	BG2	ML	BS	BL1	BL2	BG1	BG2
	AEst	0.7147	0.6932	0.6967	0.6897	0.6932	0.6591	−2.4047	−2.2673	−2.2103	−2.3252	−2.2673	−2.0368
	RMSE	0.2795	0.0910	0.0922	0.0899	0.0910	0.0909	1.4593	0.3307	0.3716	0.2948	0.3307	0.5489
S[1]	MRAB	0.3114	0.1053	0.1066	0.1042	0.1053	0.1090	0.4666	0.1085	0.1247	0.0957	0.1085	0.1885
	AL	1.2259	0.5866	0.5872	0.5873	0.5866	0.6423	6.5284	2.3994	2.4378	2.4370	2.3994	2.7169
	CP	0.952	0.993	0.992	0.992	0.994	0.997	0.964	0.999	0.998	0.994	0.995	0.992
	AEst	0.7418	0.6887	0.6925	0.6850	0.6887	0.6525	−2.6099	−2.2445	−2.1841	−2.3057	−2.2445	−1.9565
	RMSE	0.3261	0.0884	0.0895	0.0876	0.0884	0.0912	1.4679	0.3271	0.3749	0.2836	0.3271	0.6527
S[2]	MRAB	0.3728	0.1088	0.1099	0.1077	0.1088	0.1118	0.4486	0.1121	0.1309	0.0956	0.1121	0.2165
	AL	1.3553	0.6024	0.6031	0.6029	0.6024	0.6684	7.2222	2.4649	2.5124	2.5104	2.4649	2.7955
	CP	0.974	0.992	0.997	0.991	0.998	0.999	0.976	0.998	0.995	0.994	0.994	0.993
	AEst	0.7160	0.6785	0.6823	0.6748	0.6785	0.6411	−2.5443	−2.2608	−2.2015	−2.3208	−2.2608	−2.0165
	RMSE	0.3276	0.0897	0.0903	0.0892	0.0897	0.0966	1.4147	0.3234	0.3681	0.2838	0.3234	0.5638
S[3]	MRAB	0.3788	0.1098	0.1104	0.1095	0.1098	0.1174	0.4520	0.1048	0.1229	0.0890	0.1048	0.1923
	AL	1.3848	0.6062	0.6067	0.6069	0.6062	0.6714	7.1496	2.4441	2.4886	2.4827	2.4441	2.7547
	CP	0.965	0.996	0.998	0.996	0.994	0.995	0.963	0.998	0.992	0.995	0.995	0.996
	AEst	0.7163	0.6800	0.6833	0.6769	0.6800	0.6481	−2.5516	−2.2575	−2.2033	−2.3122	−2.2575	−2.0343
	RMSE	0.2975	0.0986	0.0992	0.0982	0.0986	0.1033	1.3569	0.3584	0.3959	0.3254	0.3584	0.58216
S[4]	MRAB	0.3473	0.1161	0.1165	0.1158	0.1161	0.1232	0.4489	0.1171	0.1321	0.1040	0.1171	0.1926
	AL	1.1577	0.5606	0.5611	0.5612	0.5606	0.6128	6.0597	2.3281	2.3685	2.3615	2.3281	2.6040
	CP	0.921	0.990	0.994	0.991	0.995	0.993	0.965	0.995	0.996	0.993	0.993	0.997
	AEst	0.6787	0.6613	0.6646	0.6581	0.6613	0.6284	−2.5648	−2.2896	−2.2340	−2.3460	−2.2896	−2.0787
	RMSE	0.2769	0.0859	0.0858	0.0862	0.0859	0.0979	1.3772	0.3118	0.3498	0.2793	0.3118	0.5014
S[5]	MRAB	0.3202	0.1041	0.1044	0.1041	0.1041	0.1165	0.4420	0.1055	0.1192	0.0940	0.1055	0.1723
	AL	1.1655	0.5617	0.5623	0.5622	0.5617	0.6183	6.1312	2.3575	2.3984	2.3925	2.3575	2.6548
	CP	0.975	0.994	0.992	0.999	0.996	0.993	0.988	0.996	0.993	0.994	0.995	0.995
	AEst	0.7404	0.6795	0.6828	0.6762	0.6795	0.6465	−2.7783	−2.3255	−2.2713	−2.3804	−2.3255	−2.1235
	RMSE	0.2965	0.0882	0.0887	0.0878	0.0882	0.0940	1.3210	0.2824	0.3178	0.2537	0.2824	0.4609
S[6]	MRAB	0.3435	0.1051	0.1055	0.1048	0.1051	0.1136	0.4173	0.0913	0.1031	0.0831	0.0913	0.1548
	AL	1.2550	0.5698	0.5702	0.5704	0.5698	0.6222	6.3919	2.3310	2.3682	2.3684	2.3310	2.5782
	CP	0.972	0.997	0.994	0.993	0.991	0.990	0.987	0.999	0.992	0.991	0.992	0.995
	AEst	0.6911	0.6642	0.6667	0.6616	0.6642	0.6375	−2.5575	−2.3195	−2.2696	−2.3698	−2.3195	−2.1486
	RMSE	0.2472	0.0928	0.0928	0.0929	0.0928	0.1004	1.2336	0.3301	0.3567	0.3092	0.3301	0.4567
S[7]	MRAB	0.2965	0.1129	0.1128	0.1130	0.1129	0.1209	0.4161	0.1134	0.1226	0.1063	0.1134	0.1557
	AL	0.9138	0.5076	0.5080	0.5079	0.5076	0.5444	4.9213	2.2302	2.2624	2.2672	2.2302	2.4611
	CP	0.976	0.997	0.995	0.991	0.992	0.991	0.986	0.999	0.998	0.991	0.995	0.992
	AEst	0.7063	0.6766	0.6795	0.6737	0.6766	0.6479	−2.5584	−2.3254	−2.2743	−2.3770	−2.3254	−2.1423
	RMSE	0.2333	0.0905	0.0909	0.0903	0.0905	0.0955	1.1599	0.3275	0.3567	0.3038	0.3275	0.4777
S[8]	MRAB	0.2639	0.1035	0.1038	0.1034	0.1035	0.1121	0.3614	0.1036	0.1160	0.0939	0.1036	0.1588
	AL	0.9959	0.5316	0.5321	0.5322	0.5316	0.5778	5.1950	2.2543	2.2895	2.2872	2.2543	2.4964
	CP	0.967	0.990	0.991	0.992	0.994	0.995	0.977	0.995	0.991	0.993	0.991	0.996
	AEst	0.7178	0.6785	0.6815	0.6755	0.6785	0.6492	−2.6383	−2.3430	−2.2911	−2.3954	−2.3430	−2.1496
	RMSE	0.2565	0.0884	0.0889	0.0881	0.0884	0.0929	1.3026	0.3182	0.3453	0.2976	0.3182	0.4866
S[9]	MRAB	0.2928	0.0998	0.1004	0.0994	0.0998	0.1081	0.4226	0.1070	0.1172	0.0987	0.1070	0.1592
	AL	1.0423	0.5369	0.5372	0.5373	0.5369	0.5849	5.3323	2.2717	2.3090	2.3023	2.2717	2.5390
	CP	0.969	0.991	0.995	0.999	0.997	0.999	0.962	0.994	0.999	0.991	0.996	0.997
	AEst	0.6812	0.6652	0.6676	0.6628	0.6652	0.6409	−2.4913	−2.3184	−2.2730	−2.3642	−2.3184	−2.1640
	RMSE	0.2024	0.0848	0.0847	0.0850	0.0848	0.0922	1.0922	0.3526	0.3748	0.3349	0.3526	0.4645
S[10]	MRAB	0.2449	0.0997	0.0996	0.0999	0.0997	0.1095	0.3559	0.1171	0.1254	0.1100	0.1171	0.1564
	AL	0.8285	0.4857	0.4861	0.4860	0.4857	0.5200	4.3454	2.1227	2.1469	2.1474	2.1227	2.3318
	CP	0.966	0.995	0.991	0.991	0.996	0.995	0.987	0.995	0.993	0.993	0.998	0.995
	AEst	0.6962	0.6748	0.6773	0.6723	0.6748	0.6494	−2.4852	−2.3033	−2.2567	−2.3503	−2.3033	−2.1435
	RMSE	0.2166	0.0899	0.0901	0.0898	0.0899	0.0951	1.0112	0.3180	0.3465	0.2941	0.3180	0.4446
S[11]	MRAB	0.2522	0.0985	0.0989	0.0983	0.0985	0.1065	0.3275	0.1020	0.1122	0.0945	0.1020	0.1491
	AL	0.8809	0.4995	0.4999	0.4998	0.4995	0.5364	4.5087	2.1458	2.1752	2.1735	2.1458	2.3575
	CP	0.931	0.998	0.991	0.995	0.994	0.994	0.964	0.991	0.992	0.993	0.997	0.994
	AEst	0.6855	0.6649	0.6674	0.6624	0.6649	0.6394	−2.5269	−2.3223	−2.2762	−2.3691	-2.3223	−2.1676
	RMSE	0.2125	0.0838	0.0837	0.0840	0.0838	0.0920	1.0724	0.3276	0.3523	0.3077	0.3276	0.4462
S[12]	MRAB	0.2532	0.1033	0.1032	0.1036	0.1033	0.1119	0.3420	0.1073	0.1166	0.0992	0.1073	0.1478
	AL	0.8805	0.4970	0.4972	0.4974	0.4970	0.5354	4.5205	2.1423	2.1702	2.1749	2.1423	2.3727
	CP	0.953	0.991	0.991	0.995	0.995	0.992	0.972	0.998	0.992	0.995	0.991	0.995

Table 16. Results of point and interval estimates for λ and ξ under SSPALT with the P-T-II CS.

Scheme		λ						ξ					
		ML	BS	BL1	BL2	BG1	BG2	ML	BS	BL1	BL2	BG1	BG2
S[1]	AEst	3.4942	3.5204	3.6022	3.4420	3.5204	3.3649	2.0138	1.6964	1.7062	1.6867	1.6964	1.6585
	RMSE	1.8407	0.4492	0.4223	0.4871	0.4492	0.5446	0.9892	0.1664	0.1739	0.1593	0.1664	0.1427
	MRAB	0.3996	0.0959	0.0920	0.1036	0.0959	0.1176	0.3781	0.0804	0.0846	0.0766	0.0804	0.0678
	AL	7.6730	2.8042	2.8675	2.8700	2.8042	3.0368	3.3215	0.9808	0.9835	0.9832	0.9808	1.0216
	CP	0.939	0.996	0.994	0.992	0.995	0.995	0.986	0.995	0.992	0.991	0.994	0.999
S[2]	AEst	3.8325	3.5984	3.6850	3.5156	3.5984	3.4377	1.8509	1.6858	1.6954	1.6764	1.6858	1.6487
	RMSE	1.6439	0.3646	0.3476	0.4000	0.3646	0.4538	0.7804	0.1586	0.1657	0.1519	0.1586	0.1366
	MRAB	0.3394	0.0808	0.0753	0.0899	0.0808	0.1026	0.2678	0.0775	0.0812	0.0740	0.0775	0.0666
	AL	8.3754	2.8774	2.9372	2.9578	2.8774	3.1115	2.8802	0.9689	0.9712	0.9718	0.9689	1.0184
	CP	0.979	0.993	0.999	0.993	0.996	0.998	0.985	0.996	0.995	0.992	0.998	0.996
S[3]	AEst	3.7474	3.6106	3.6949	3.5296	3.6106	3.4540	1.9743	1.7047	1.7144	1.6953	1.7047	1.6679
	RMSE	1.5803	0.4226	0.4133	0.4470	0.4226	0.4946	1.0342	0.1898	0.1970	0.1829	0.1898	0.1672
	MRAB	0.3361	0.0972	0.0937	0.1031	0.0972	0.1136	0.3501	0.0941	0.0983	0.0902	0.0941	0.0818
	AL	8.1567	2.8489	2.9064	2.9118	2.8489	3.0713	3.0672	0.9699	0.9730	0.9722	0.9699	1.0123
	CP	0.984	0.993	0.993	0.993	0.998	0.994	0.966	0.998	0.996	0.991	0.992	0.997
S[4]	AEst	3.8128	3.5589	3.6329	3.4872	3.5589	3.4179	1.7087	1.6470	1.6548	1.6394	1.6470	1.6163
	RMSE	1.4446	0.3868	0.3633	0.4214	0.3868	0.4720	0.5864	0.1433	0.1476	0.1394	0.1433	0.1319
	MRAB	0.3152	0.0850	0.0803	0.0928	0.0850	0.1048	0.2163	0.0712	0.0730	0.0696	0.0712	0.0668
	AL	6.8981	2.6763	2.7226	2.7307	2.6763	2.8896	2.1408	0.8730	0.8746	0.8755	0.8730	0.9052
	CP	0.985	0.998	0.998	0.993	0.998	0.996	0.969	0.991	0.996	0.991	0.998	0.995
S[5]	AEst	3.9034	3.6261	3.7025	3.5520	3.6261	3.4827	1.6826	1.6494	1.6571	1.6418	1.6494	1.6189
	RMSE	1.5707	0.3890	0.3770	0.4139	0.3890	0.4585	0.4212	0.1407	0.1452	0.1365	0.1407	0.1282
	MRAB	0.3354	0.0865	0.0830	0.0932	0.0865	0.1040	0.2003	0.0727	0.0747	0.0709	0.0727	0.0676
	AL	6.9845	2.7250	2.7772	2.7864	2.7250	2.9035	1.9188	0.8693	0.8707	0.8715	0.8693	0.9034
	CP	0.966	0.994	0.992	0.992	0.992	0.991	0.973	0.996	0.994	0.993	0.990	0.998
S[6]	AEst	4.0600	3.6473	3.7216	3.5752	3.6473	3.5092	1.6934	1.6802	1.6882	1.6723	1.6802	1.6491
	RMSE	1.4370	0.3583	0.3518	0.3790	0.3583	0.4188	0.3693	0.1538	0.1594	0.1485	0.1538	0.1363
	MRAB	0.3039	0.0767	0.0742	0.0820	0.0767	0.0919	0.1827	0.0754	0.0783	0.0726	0.0754	0.0665
	AL	7.1242	2.6766	2.7289	2.7217	2.6766	2.8674	1.8418	0.8869	0.8883	0.8887	0.8869	0.9183
	CP	0.974	0.992	0.993	0.997	0.991	0.996	0.969	0.997	0.99	0.996	0.995	0.993
S[7]	AEst	3.8253	3.6156	3.6852	3.5480	3.6156	3.4854	1.7039	1.6662	1.6733	1.6593	1.6662	1.6385
	RMSE	1.3884	0.3567	0.3430	0.3822	0.3567	0.4238	0.4077	0.1465	0.1511	0.1422	0.1465	0.1326
	MRAB	0.2987	0.0764	0.0732	0.0829	0.0764	0.0935	0.1821	0.0733	0.0757	0.0710	0.0733	0.0664
	AL	5.7268	2.5952	2.6388	2.6481	2.5952	2.7603	1.6380	0.8353	0.8371	0.8353	0.8353	0.8615
	CP	0.988	0.997	0.995	0.997	0.991	0.996	0.961	0.992	0.993	0.990	0.997	0.996
S[8]	AEst	3.7959	3.6143	3.6827	3.5477	3.6143	3.4857	1.7723	1.6896	1.6968	1.6896	1.6896	1.6620
	RMSE	1.3678	0.3955	0.3847	0.4170	0.3955	0.4552	0.5269	0.1774	0.1823	0.1726	0.1774	0.1619
	MRAB	0.2887	0.0804	0.0788	0.0860	0.0804	0.0959	0.2224	0.0865	0.0887	0.0843	0.0865	0.0799
	AL	5.8926	2.5819	2.6315	2.6352	2.5819	2.7502	1.7315	0.8391	0.8406	0.8408	0.8391	0.8665
	CP	0.952	0.991	0.990	0.995	0.997	0.998	0.977	0.995	0.993	0.991	0.991	0.997
S[9]	AEst	3.8586	3.6007	3.6689	3.6005	3.6007	3.4707	1.7199	1.6770	1.6840	1.6700	1.6770	1.6496
	RMSE	1.4872	0.4059	0.3909	0.4308	0.4059	0.4732	0.4087	0.1595	0.1641	0.1550	0.1595	0.1449
	MRAB	0.3111	0.0846	0.0802	0.0924	0.0846	0.1039	0.1992	0.0785	0.0807	0.0765	0.0785	0.0720
	AL	5.9697	2.579	2.6238	2.6243	2.5790	2.7363	1.6694	0.8325	0.8338	0.8344	0.8325	0.8617
	CP	0.954	0.994	0.991	0.992	0.993	0.992	0.961	0.990	0.992	0.991	0.997	0.992
S[10]	AEst	3.8108	3.6382	3.6993	3.5783	3.6382	3.5232	1.6553	1.6446	1.6502	1.6390	1.6446	1.6220
	RMSE	1.2517	0.3956	0.3874	0.4125	0.3956	0.4451	0.3124	0.1300	0.1331	0.1271	0.1300	0.1210
	MRAB	0.2681	0.0858	0.083	0.0896	0.0858	0.0970	0.1488	0.0659	0.0677	0.0643	0.0659	0.0615
	AL	4.9417	2.4380	2.4821	2.4847	2.4380	2.5774	1.3104	0.7482	0.7493	0.7494	0.7482	0.7697
	CP	0.969	0.997	0.992	0.991	0.992	0.997	0.966	0.995	0.995	0.991	0.997	0.992
S[11]	AEst	3.7240	3.5605	3.6210	3.5011	3.5605	3.4441	1.6609	1.6509	1.6565	1.6453	1.6509	1.6285
	RMSE	1.1359	0.4074	0.3879	0.4340	0.4074	0.4742	0.2986	0.1454	0.1486	0.1424	0.1454	0.1364
	MRAB	0.2403	0.0844	0.0789	0.0922	0.0844	0.1035	0.1492	0.0702	0.0718	0.0688	0.0702	0.0659
	AL	5.0011	2.4272	2.4633	2.4644	2.4272	2.5868	1.2827	0.7479	0.7490	0.7490	0.7479	0.7664
	CP	0.953	0.992	0.991	0.995	0.993	0.995	0.968	0.992	0.995	0.996	0.994	0.992
S[12]	AEst	3.8154	3.6087	3.6696	3.5493	3.6087	3.4943	1.6515	1.6519	1.6575	1.6464	1.6519	1.6297
	RMSE	1.2039	0.3991	0.3858	0.42034	0.3991	0.4562	0.2909	0.1417	0.1448	0.1388	0.1417	0.1326
	MRAB	0.2606	0.0858	0.0832	0.0900	0.0858	0.0974	0.1472	0.0706	0.0721	0.0694	0.0706	0.0671
	AL	5.0425	2.4375	2.4727	2.4830	2.4375	2.5834	1.2778	0.7433	0.7445	0.7447	0.7433	0.7638
	CP	0.976	0.995	0.997	0.993	0.994	0.996	0.988	0.995	0.996	0.995	0.995	0.993

Table 17. Results of point and interval estimates for $R(t = 1.02)$ and $h(t = 1.02)$ under SSPALT with the P-T-II CS.

Scheme		$R(t = 1.02)$						$h(t = 1.02)$					
		ML	BS	BL1	BL2	BG1	BG2	ML	BS	BL1	BL2	BG1	BG2
S[1]	AEst	0.4815	0.4582	0.4589	0.4576	0.4582	0.4478	3.5173	3.5358	3.6176	3.4593	3.5358	3.3931
	RMSE	0.0787	0.0616	0.0615	0.0618	0.0616	0.0660	0.9550	0.7120	0.7699	0.6656	0.7120	0.6598
	MRAB	0.1345	0.1076	0.1073	0.1080	0.1076	0.1158	0.2140	0.1683	0.1797	0.1601	0.1683	0.1605
	AL	0.3192	0.2592	0.2593	0.2593	0.2592	0.2697	3.1953	2.7331	2.7866	2.8066	2.7331	2.9574
	CP	0.951	0.992	0.991	0.995	0.996	0.995	0.984	0.992	0.996	0.994	0.994	0.998
S[2]	AEst	0.4628	0.4432	0.4439	0.4425	0.4432	0.4319	3.6618	3.6773	3.7611	3.5988	3.6773	3.5366
	RMSE	0.0764	0.0664	0.0661	0.0667	0.0664	0.0730	0.8939	0.7353	0.8079	0.6734	0.7353	0.6548
	MRAB	0.1304	0.1110	0.1105	0.1114	0.1110	0.1211	0.1921	0.1634	0.1790	0.1500	0.1634	0.1469
	AL	0.3246	0.2659	0.2660	0.2660	0.2659	0.2779	3.2013	2.777	2.8375	2.8486	2.777	2.9936
	CP	0.964	0.992	0.991	0.990	0.991	0.994	0.969	0.992	0.993	0.992	0.996	0.995
S[3]	AEst	0.4736	0.4498	0.4505	0.4491	0.4498	0.4389	3.7357	3.7049	3.7892	3.6259	3.7049	3.5665
	RMSE	0.0883	0.0705	0.0703	0.0709	0.0705	0.0758	1.1587	0.8918	0.9661	0.8276	0.8918	0.8133
	MRAB	0.1515	0.1243	0.1238	0.1248	0.1243	0.1351	0.2459	0.1976	0.2109	0.1866	0.1976	0.1860
	AL	0.3226	0.2637	0.2637	0.2638	0.2637	0.2752	3.2588	2.7626	2.8202	2.8438	2.7626	2.9706
	CP	0.961	0.992	0.991	0.991	0.995	0.991	0.958	0.990	0.992	0.995	0.991	0.998
S[4]	AEst	0.4653	0.4552	0.4557	0.4549	0.4552	0.4476	3.4268	3.4717	3.5216	3.4238	3.4717	3.3808
	RMSE	0.0720	0.0615	0.0614	0.0616	0.0615	0.0647	0.6293	0.5705	0.6007	0.5452	0.5705	0.5419
	MRAB	0.1232	0.1064	0.1062	0.1066	0.1064	0.1126	0.1403	0.1265	0.1309	0.1236	0.1265	0.1251
	AL	0.2625	0.2224	0.2224	0.2224	0.2224	0.2289	2.4090	2.1752	2.2023	2.2119	2.1752	2.2798
	CP	0.982	0.992	0.995	0.993	0.995	0.992	0.952	0.993	0.997	0.993	0.998	0.993
S[5]	AEst	0.4694	0.4589	0.4594	0.4584	0.4589	0.4513	3.5067	3.5218	3.5707	3.4746	3.5218	3.4334
	RMSE	0.0596	0.0485	0.0484	0.0486	0.0485	0.0516	0.6389	0.5666	0.5988	0.5390	0.5666	0.5317
	MRAB	0.1036	0.0834	0.0832	0.0835	0.0834	0.0873	0.1403	0.1268	0.1331	0.1210	0.1268	0.1196
	AL	0.2654	0.2250	0.2251	0.2251	0.2250	0.2320	2.3523	2.1617	2.1893	2.1909	2.1617	2.2736
	CP	0.982	0.994	0.997	0.998	0.994	0.993	0.951	0.994	0.996	0.997	0.991	0.993
S[6]	AEst	0.4666	0.4560	0.4565	0.4555	0.4560	0.4484	3.5820	3.5943	3.6459	3.5446	3.5943	3.5034
	RMSE	0.0681	0.0577	0.0576	0.0578	0.0577	0.0609	0.7261	0.6440	0.6827	0.6097	0.6440	0.5994
	MRAB	0.1211	0.0997	0.0996	0.0998	0.0997	0.1043	0.1568	0.1439	0.1523	0.1365	0.1439	0.1342
	AL	0.2641	0.2242	0.2242	0.2242	0.2242	0.2314	2.4155	2.2102	2.2405	2.2494	2.2102	2.3228
	CP	0.977	0.996	0.996	0.995	0.996	0.993	0.973	0.997	0.993	0.993	0.994	0.993
S[7]	AEst	0.4748	0.4659	0.4663	0.4655	0.4659	0.4600	3.4669	3.4876	3.5257	3.4505	3.4876	3.4173
	RMSE	0.0622	0.0525	0.0525	0.0526	0.0525	0.0541	0.5097	0.4861	0.5087	0.4667	0.4861	0.4610
	MRAB	0.1071	0.0905	0.0904	0.0905	0.0905	0.0930	0.1146	0.1091	0.1136	0.1058	0.1091	0.1054
	AL	0.2297	0.1988	0.1988	0.1988	0.1988	0.2030	2.0515	1.9191	1.9403	1.9432	1.9191	1.9992
	CP	0.966	0.997	0.992	0.991	0.995	0.994	0.986	0.991	0.997	0.991	0.993	0.992
S[8]	AEst	0.4727	0.4620	0.4624	0.4616	0.4620	0.4561	3.5305	3.5439	3.5825	3.5064	3.5439	3.4741
	RMSE	0.0691	0.0585	0.0584	0.0586	0.0585	0.0604	0.5950	0.5557	0.5809	0.5334	0.5557	0.5254
	MRAB	0.1189	0.1018	0.1017	0.1019	0.1018	0.1045	0.1430	0.1341	0.1393	0.1295	0.1341	0.1278
	AL	0.2291	0.1995	0.1995	0.1995	0.1995	0.2042	2.0774	1.9323	1.9536	1.9569	1.9323	2.0083
	CP	0.970	0.994	0.994	0.996	0.994	0.994	0.976	0.996	0.998	0.992	0.991	0.995
S[9]	AEst	0.4750	0.4665	0.4669	0.4661	0.4665	0.4606	3.4627	3.4708	3.5072	3.4355	3.4708	3.4034
	RMSE	0.0561	0.0467	0.0467	0.0467	0.0467	0.0482	0.5327	0.4829	0.5024	0.4662	0.4829	0.4621
	MRAB	0.0936	0.0803	0.0802	0.0805	0.0803	0.0837	0.1256	0.1146	0.1188	0.1109	0.1146	0.1103
	AL	0.2298	0.2003	0.2003	0.2003	0.2003	0.2046	2.0062	1.8777	1.8967	1.89947	1.8777	1.9498
	CP	0.961	0.996	0.995	0.995	0.996	0.996	0.958	0.994	0.996	0.990	0.992	0.997
S[10]	AEst	0.4640	0.4595	0.4598	0.4593	0.4595	0.4554	3.4753	3.4855	3.5105	3.4609	3.4855	3.4388
	RMSE	0.0457	0.0407	0.0407	0.0408	0.0407	0.0424	0.4354	0.4138	0.4283	0.4009	0.4138	0.3960
	MRAB	0.0791	0.0698	0.0697	0.0699	0.0698	0.0725	0.0964	0.0929	0.0960	0.0901	0.0929	0.0889
	AL	0.1880	0.1673	0.1673	0.1673	0.1673	0.1701	1.6424	1.5677	1.5776	1.5810	1.5677	1.6056
	CP	0.976	0.996	0.993	0.991	0.996	0.993	0.973	0.992	0.995	0.99	0.996	0.992
S[11]	AEst	0.4701	0.4643	0.4646	0.4640	0.4643	0.4603	3.3946	3.4082	3.4319	3.3848	3.4082	3.3629
	RMSE	0.0485	0.0413	0.0412	0.0413	0.0413	0.0424	0.4753	0.4461	0.4559	0.4377	0.4461	0.4371
	MRAB	0.0841	0.0700	0.0699	0.0701	0.0700	0.0725	0.1080	0.1022	0.1046	0.1001	0.1022	0.0998
	AL	0.1877	0.1673	0.1673	0.1673	0.1673	0.1702	1.5911	1.5267	1.5364	1.5374	1.5267	1.5686
	CP	0.966	0.997	0.994	0.996	0.993	0.996	0.961	0.994	0.994	0.997	0.995	0.996
S[12]	AEst	0.4703	0.4656	0.4659	0.4653	0.4656	0.4617	3.4357	3.4430	3.4668	3.4196	3.4430	3.3979
	RMSE	0.0492	0.04152	0.0415	0.0416	0.0415	0.0426	0.4219	0.3997	0.4106	0.3902	0.3997	0.3874
	MRAB	0.0849	0.0711	0.0711	0.0712	0.0711	0.0726	0.0997	0.0956	0.0992	0.0925	0.0956	0.0909
	AL	0.1878	0.1664	0.1664	0.1664	0.1664	0.1692	1.6027	1.5317	1.5415	1.5421	1.5317	1.5719
	CP	0.956	0.996	0.992	0.992	0.997	0.996	0.975	0.997	0.994	0.994	0.994	0.995

7. Conclusions

The paper derives extensive ML and Bayesian inference algorithms of the QHRD under SSPALT with progressive Type-II censoring and binomial removals. The proposed model incorporates the TRV model as well as the flexibility of censoring to provide the correct estimation of the model parameters, the acceleration factor, and important measures of reliability of the model. The results of the simulation testify to the strength, versatility, and real-life applicability of the approach. The QHRD demonstrates competitive and mostly better goodness-of-fit than other lifetime models. Future studies can build this framework for multistep or continuously varying stress mechanisms based on different censoring schemes and the best test design strategies to make them cost-efficient. Other extensions may be a regression-like extension that admits covariates, robustness analysis in the event of model misspecification, and a multicomponent system, such as competing risks. These extensions would also improve the applicability of the suggested methodology in contemporary reliability engineering situations.

Author contributions

Conceptualization, H. H. A., M. N. M., and M. M. M. M. Methodology, M. N. M., M. M. M. M., and M. E. M. Software, M. N. M. Validation, H. H. A., M. N. M., and N. Y. Formal analysis, H. H. A., M. N. M., M. E. M., and M. M. M. M. Investigation, M. E. M. and N. Y. Resources, H. H. A. and M. N. M. Data curation, M. E. M. and N. Y. Supervision, N. Y. and M. M. M. M. Writing—original draft preparation, H. H. A., M. N. M., and M. M. M. M. Writing—review and editing, H. H. A., M. N. M., M. E. M., N. Y., and M. M. M. M. Funding acquisition, H. H. A. All authors have read and agreed to the published version of the manuscript.

Use of Generative-AI tools declaration

The authors declare that they have not used Artificial Intelligence (AI) tools in the creation of this article.

Funding

This work was supported by the Deanship of Scientific Research, Vice Presidency for Graduate Studies and Scientific Research, King Faisal University, Saudi Arabia [Grant No. KFU261148].

Conflict of interest

All authors declare no conflicts of interest in this paper.

References

1. S. Bessler, H. Chernoff, A. W. Marshall, An optimal sequential accelerated life test, *Technometrics*, **4** (1962), 367–379. http://dx.doi.org/10.1080/00401706.1962.10490019
2. H. Chernoff, Optimal accelerated life designs for estimation, *Technometrics*, **4** (1962), 381–408. http://dx.doi.org/10.1080/00401706.1962.10490020
3. W. Nelson, *Accelerated testing: Statistical models, test plans and data analysis*, New York: Wiley, 1990. http://dx.doi.org/10.1002/9780470316795
4. W. Q. Meeker, L. A. Escobar, C. J. Lu, Accelerated degradation tests: Modeling and analysis, *Technometrics*, **40** (1998), 89–99. http://dx.doi.org/10.1080/00401706.1998.10485191
5. D. Han, T. Bai, Design optimization of a simple step-stress accelerated life test: Contrast between continuous and interval inspections with non-uniform step durations, *Reliab. Eng. Syst. Safe.*, **199** (2020), 106875. http://dx.doi.org/10.1016/j.ress.2020.106875
6. A. Rahman, T. N. Sindhu, S. A. Lone, M. Kamal, Statistical inference for Burr type X distribution using geometric process in accelerated life testing design for time censored data, *Pak. J. Stat. Oper. Res.*, **16** (2020), 577–586. http://dx.doi.org/10.18187/pjsor.v16i3.2252
7. S. J. Wu, Estimation of the parameters of the Weibull distribution with progressively censored data, *J. Japan Statist. Soc.*, **32** (2002), 155–163. http://dx.doi.org/10.14490/jjss.32.155
8. E. A. Ahmed, Estimation of some lifetime parameters of generalized Gompertz distribution under progressively type-II censored data, *Appl. Math. Model.*, **39** (2015), 5567–5578. http://dx.doi.org/10.1016/j.apm.2015.01.023
9. M. A. W. Mahmoud, D. A. Ramadan, M. M. M. Mansour, Estimation of lifetime parameters of the modified extended exponential distribution with application to a mechanical model, *Commun. Stat. Simul. C.*, **51** (2022), 7005–7018. http://dx.doi.org/10.1080/03610918.2020.1821887
10. L. Wang, K. Wu, X. Zuo, Inference and prediction of progressive Type-II censored data from Unit-Generalized Rayleigh distribution, *Hacet. J. Math. Stat.*, **51** (2022), 1752–1767. http://dx.doi.org/10.15672/hujms.988054
11. D. A. Ramadan, Y. A. Tashkandy, M. E. Bakr, O. S. Balogun, M. M. Hasaballah, Analysis of Marshall-Olkin extended Gumbel type-II distribution under progressive type-II censoring with applications, *AIP Adv.*, **14** (2024), 055137. http://dx.doi.org/10.1063/5.0210905
12. Y. Tashkandy, E. Almetwally, R. Ragab, A. Gemeay, M. A. El-Raouf, S. Khosa, et al., Statistical inferences for the extended inverse Weibull distribution under progressive type-II censored sample with applications, *Alex. Eng. J.*, **65** (2023), 493–502. http://dx.doi.org/10.1016/j.aej.2022.09.023
13. H. Haj Ahmad, Best prediction method for progressive Type-II censored samples under new Pareto model with applications, *J. Math.*, **2021** (2021), 1355990. http://dx.doi.org/10.1155/2021/1355990
14. O. E. Abo-Kasem, A. R. El Saeed, A. I. El Sayed, Optimal sampling and statistical inferences for Kumaraswamy distribution under progressive type-II censoring schemes, *Sci. Rep.*, **13** (2023), 12063. http://dx.doi.org/10.1038/s41598-023-38594-9

15. D. S. Bai, S. W. Chung, Y. R. Chun, Optimal design of partially accelerated life tests for the lognormal distribution under type I censoring, *Reliab. Eng. Syst. Saf.*, **40** (1993), 85–92. http://dx.doi.org/10.1016/0951-8320(93)90122-F

16. A. Rahman, S. Lone, A. Islam, Analysis of exponentiated exponential model under step stress partially accelerated life testing plan using progressive type-II censored data, *Investigacion Operacional*, **39** (2018), 551–559.

17. R. M. El-Sagheer, M. A. W. Mahmoud, M. M. M. Mansour, Inferences for Weibull-Gamma distribution in presence of partially accelerated life test, *J. Stat. Appl. Probab.*, **9** (2020), 93–107. http://dx.doi.org/10.18576/jsap/090109

18. I. Alam, S. Anwar, L. K. Sharma, Inference on adaptive Type-II progressive hybrid censoring under partially accelerated life test for Gompertz distribution, *Int. J. Syst. Assur. Eng. Manag.*, **14** (2023), 2661–2673. http://dx.doi.org/10.1007/s13198-023-02129-2

19. L. A. Al-Essa, A. H. Abdel-Hamid, T. Alballa, A. Hashem, Reliability analysis of the triple modular redundancy system under step-partially accelerated life tests using Lomax distribution, *Sci. Rep.*, **13** (2023), 14719. http://dx.doi.org/10.1038/s41598-023-41363-3

20. M. M. Yousef, R. Alsultan, S. G. Nassr, Parametric inference on partially accelerated life testing for the inverted Kumaraswamy distribution based on Type-II progressive censoring data, *Math. Biosci. Eng.*, **20** (2023), 1674–1694. http://dx.doi.org/10.3934/mbe.2023076

21. I. Alam, A. Ahmed, Parametric and interval estimation under step-stress partially accelerated life tests using adaptive Type-II progressive hybrid censoring, *Ann. Data. Sci.*, **10** (2023), 441–453. https://doi.org/10.1007/s40745-020-00249-1

22. M. M. Yousef, A. Fayomi, E. M. Almetwally, Simulation techniques for strength component partially accelerated to analyze stress-strength model, *Symmetry*, **15** (2023), 1183. http://dx.doi.org/10.3390/sym15061183

23. Y. Tian, W. Gui, Inference and expected total test time for step-stress life test in the presence of complementary risks and incomplete data, *Comput. Stat.*, **39** (2024), 1023–1060. http://dx.doi.org/10.1007/s00180-023-01343-7

24. H. H. Ahmad, D. A. Ramadan, E. M. Almetwally, Tampered random variable analysis in step-stress testing: Modeling, inference, and applications, *Mathematics*, **12** (2024), 1248. http://dx.doi.org/10.3390/math12081248

25. L. J. Bain, Analysis for the linear failure-rate life-testing distribution, *Technometrics*, **16** (1974), 551–559. http://dx.doi.org/10.1080/00401706.1974.10489237

26. I. Elbatal, N. Butt, A new generalization of quadratic hazard rate distribution, *Pak. J. Stat. Oper. Res.*, **9** (2013), 4.

27. A. Mustafa, A new bivariate distribution with generalized quadratic hazard rate marginals, *J. Math. Stat.*, **12** (2016), 255–270.

28. F. Bhatti, G. Hamedani, W. Sheng, M. Ahmad, On extended quadratic hazard rate distribution: Development, properties, characterizations and applications, *Stoch. Qual. Contr.*, **33** (2018), 45–60. http://dx.doi.org/10.1515/eqc-2018-0002

29. F. Merovci, I. Elbatal, The beta quadratic hazard rate distribution, *Pak. J. Statist.*, **31** (2015), 427–446.

30. H. Okasha, M. Kayid, A. Abouammoh, I. Elbatal, A new family of quadratic hazard rate-geometric distributions with reliability applications, *J. Test. Eval.*, **44** (2016), 1397–1948. http://dx.doi.org/10.1520/JTE20150116

31. A. Al-Hossain, J. Dar, Some results on moment of order statistics for the quadratic hazard rate distribution, *J. Stat. Appl. Pro.*, **5** (2016), 371–376. http://dx.doi.org/10.18576/jsap/050218

32. M. Nagy, A. H. Mansi, M. N. Mousa, M. E. Moshref, N. Youns, M. M. M. Mansour, On estimation of the quadratic hazard rate model parameters: Simulation and application, *AIP Adv.*, **15** (2025), 055126. http://dx.doi.org/10.1063/5.0257356

33. M. N. Mousa, M. E. Moshref, N. Youns, M. M. M. Mansour, Inference under hybrid censoring for the quadratic hazard rate model: Simulation and applications to COVID-19 mortality, *Mod. J. Stat.*, **2** (2025), 1–31. http://dx.doi.org/10.64389/mjs.2026.02113

34. P. K. Goel, *Some estimation problems in the study of tampered random variables*, Carnegie Mellon University, 1971.

35. N. Balakrishnan, R. Aggarwala, *Progressive censoring: Theory, methods and applications*, New York: Springer, 2000. http://dx.doi.org/10.1007/978-1-4612-1334-5

36. N. Balakrishnan, E. Cramer, *The art of progressive censoring: Applications to reliability and quality*, New York: Springer, 2014. http://dx.doi.org/10.1007/978-0-8176-4807-7

37. N. Balakrishnan, Progressive censoring methodology: An appraisal, *TEST*, **16** (2007), 211–259. http://dx.doi.org/10.1007/s11749-007-0061-y

38. S. K. Tse, C. Yang, H. K. Yuen, Statistical analysis of Weibull distributed lifetime data under type II progressive censoring with binomial removals, *J. Appl. Stat.*, **27** (2000), 1033–1043. http://dx.doi.org/10.1080/02664760050173355

39. A. Azzalini, *Statistical inference based on the likelihood*, London: Chapman & Hall, 1996. http://dx.doi.org/10.1201/9780203738627

40. S. R. Eliason, *Maximum likelihood estimation: Logic and practice*, SAGE Publications, 1993. http://dx.doi.org/10.4135/9781412984928

41. L. Held, D. Sabanés Bové, *Applied statistical inference: Likelihood and bayes*, Berlin: Springer, 2020. http://dx.doi.org/10.1007/978-3-642-37887-4

42. A. Zellner, Bayesian estimation and prediction using asymmetric loss functions, *J. Am. Stat. Assoc.*, **81** (1986), 446–451. http://dx.doi.org/10.1080/01621459.1986.10478289

43. R. Calabria, G. Pulcini, An engineering approach to Bayes estimation for the Weibull distribution, *Microelectron. Reliab.*, **34** (1994), 789–802. http://dx.doi.org/10.1016/0026-2714(94)90004-3

44. S. M. Lynch, *Introduction to applied Bayesian statistics and estimation for social scientists*, New York: Springer, 2007. http://dx.doi.org/10.1007/978-0-387-71265-9

45. L. Tierney, Markov chains for exploring posterior distributions, *Ann. Statist.*, **22** (1994), 1701–1728. http://dx.doi.org/10.1214/aos/1176325750

46. W. R. Gilks, S. Richardson, D. Spiegelhalter, *Markov chain Monte Carlo in Practice*, New York: Chapman & Hall/CRC, 1995. http://dx.doi.org/10.1201/b14835

47. Z. F. Jaheen, Empirical Bayes inference for generalized exponential distribution based on records, *Commun. Stat. Theor. M.*, **33** (2004), 1851–1861. http://dx.doi.org/10.1081/STA-120037445

48. S. Dey, S. Singh, Y. M. Tripathi, A. Asgharzadeh, Estimation and prediction for a progressively censored generalized inverted exponential distribution, *Stat. Methodol.*, **32** (2016), 185–202. http://dx.doi.org/10.1016/j.stamet.2016.05.007

49. S. Singh, Y. Tripathi, Estimating the parameters of an inverse Weibull distribution under progressive type-I interval censoring, *Stat. Papers*, **59** (2018), 21–56. http://dx.doi.org/10.1007/s00362-016-0750-2

50. S. L. Lohr, *Sampling: Design and analysis*, New York: Chapman & Hall/CRC, 2021. http://dx.doi.org/10.1201/9780429298899

51. W. H. Greene, Econometric analysis, *Stat. Papers*, **52** (2011), 983–984. http://dx.doi.org/10.1007/s00362-010-0315-8

52. L. Al-Essa, A. Abdel-Hamid, T. Alballa, A. Hashem, Reliability analysis of the triple modular redundancy system under step-partially accelerated life tests using Lomax distribution, *Sci. Rep.*, **13** (2023), 14719. http://dx.doi.org/10.1038/s41598-023-41363-3

53. M. A. Amleh, M. Z. Raqab, Inference for step-stress plan with Khamis-Higgins model under type-II censored Weibull data, *Qual. Reliab. Eng. Int.*, **39** (2023), 982–1000. http://dx.doi.org/10.1002/qre.3275

AIMS Press